ATLANTA'S URBAN HEAT ISLAND UNDER EXTREME HEAT CONDITIONS AND POTENTIAL MITIGATION STRATEGIES

by

YAN ZHOU

(Under the Direction of J. Marshall Shepherd)

ABSTRACT

The urban heat island (hereafter "UHI"), together with summertime heat waves, foster biophysical hazards such as heat stress, air pollution and associated public health problems. Mitigation strategies such as increased vegetative cover and higher albedo surface materials have been proposed. Atlanta, GA is often affected by extreme heat, and has recently been investigated to better understand its heat island and related weather modifications. The objectives of this thesis were to (1) characterize temporal variations in magnitude of the UHI around Metro Atlanta area, (2) identify climatological attributes of the UHI under extreme high temperature conditions during Atlanta's summer (Jun, July, and Aug) period, and (3) conduct theoretical numerical simulations to quantify the first-order effects of proposed mitigation strategies. Over the period 1984-2007, the climatological mean UHI magnitude for Atlanta-Athens and Athens-Monticello was 1.31^{o}C and 1.71^{o}C, respectively. There were stastically-signifcant minimum temperature trends of 0.70^{o}C per decade at Athens and -1.79^{o}C per decade at Monticello while Atlanta's minimum temperature remained unchanged. The largest (smallest) UHI magnitudes were in spring (summer) and may be coupled to cloud-radiative cycles.

Heat waves in Atlanta occurred during 50% of the years spanning 1984-2007 and were exclusively summertime phenomena. The mean number of heat wave events in Atlanta during a given heat wave year was 1.83. On average, Atlanta heat waves lasted 14.18 days although there was quite a bit of variability (standard deviation of 9.89). The mean maximum temperature during Atlanta's heat waves was 35.85° C. The Atlanta-Athens UHI was not statistically larger during a heat wave although the Atlanta-Monticello UHI was.

Model simulations captured daytime and nocturnal UHIs under heat wave conditions. Sensitivity results suggested that a 100% increase in Atlanta's surface vegetation or a tripling of its albedo effectively reduced UHI surface temperature. However, from a mitigation and technological standpoint, there is low feasibility of tripling albedo in the foreseeable future. Increased vegetation seems to be a more likely choice for mitigating surface temperature.

INDEX WORDS: Urban heat island, Heat wave, Mitigation strategies

ATLANTA'S URBAN HEAT ISLAND UNDER EXTREME HEAT CONDITIONS AND POTENTIAL MITIGATION STRATEGIES

by

YAN ZHOU

B.S., Zhejiang University, China, 2006

A Thesis Submitted to the Graduate Faculty of The University of Georgia in Partial Fulfillment of the Requirements for the Degree

MASTER OF SCIENCE

ATHENS, GEORGIA

ATLANTA'S URBAN HEAT ISLAND UNDER EXTREME HEAT CONDITIONS AND POTENTIAL MITIGATION STRATEGIES

by

YAN ZHOU

Major Professor:	J. Marshall Shepherd
Committee:	Thomas L. Mote
	Andrew J. Grundstein

Electronic Version Approved:

Maureen Grasso
Dean of the Graduate School
The University of Georgia
August, 2008

DEDICATION

This thesis is dedicated to my dear parents. Thank you for raising me up with all the unconditional love, patient, and help. You taught me how to face challenges with faith and courage. Without your support, I cannot study abroad, let alone receive a M.S. degree. Always love you!

ACKNOWLEDGEMENTS

This thesis would not have been possible without the support and encouragement of many people, especially my major professor, Dr. J. Marshall Shepherd. It is difficult to overstate my gratitude because he first brought me into the world of research. He helps me in every step of the entire process, from choosing a topic to formatting the thesis. He also provides an assistantship to support my study during 2008 summer.

I would also like to thank my committee members, Dr. Thomas L. Mote and Dr. Andrew J. Grundstein. They have taught me classes and given me lots of insightful comments on this thesis.

I cannot end without thanking my department for offering me the Teaching Assistantship, which has supported me during the two years of M.S study.

TABLE OF CONTENTS

Page

LIST OF TABLES

Page

LIST OF FIGURES

Page

CHAPTER 1

Introduction

The urban heat island (hereafter "UHI"), together with summertime heat waves, foster biophysical hazards such as heat stress, air pollution and associated public health problems. Implementation of UHI mitigation strategies such as increased vegetative cover and higher-albedo surface materials may reduce the impacts of these hazards. Since local impacts of global climate change may be intensified with UHIs, such strategies would play an important role as the public adapts to climate changes (Solecki et al. 2005). Atlanta is a rapidly urbanizing city that has recently been investigated to better understand its heat island (Quattrochi et al. 1998; Quattrochi et al. 1999; Haffner and Kidder 1999; Taha 1999) and urban-related weather modifications (Bornstein; Lin 2000; Dixon and Mote 2003; Shepherd et al. 2002; Mote et al. 2007).

In this thesis study, the overarching objectives are to (1) characterize annual and seasonal variations in magnitude of the UHI around the Metro Atlanta area, (2) identify climatological attributes of the UHI under extreme high temperature conditions (i.e., heat waves) during Atlanta's summer (June, July, and August) period, and (3) conduct theoretical numerical simulations to quantify the first-order effects of proposed mitigation strategies (e.g. albedo surfaces and greening) on UHI intensity.

1.1 Hazardous heat waves

The Fourth Assessment Report of the IPCC (2007) warned that "It is very likely that hot extremes, heat waves, and heavy precipitation events will continue to become more frequent". Sterl et al. (2008) used an ensemble model approach for the IPCC A1b scenario to investigate extremely high surface temperatures. They found that extreme temperatures, in terms of 100-year return values, will increase faster than global mean temperatures. Heat waves, on average, cause the most deaths annually compared to any other natural catastrophes (Changnon et al. 1996), as evident by the 1995 heat wave in the Midwestern United States and the heat wave that occurred in many European countries during the summer of 2003.

The 1995 heat wave in United States was responsible for more than 830 deaths nationally, with 525 of these in Chicago, IL (Changnon et al. 1996) (Figure 1). During the second half of July 1999, a heat wave in the Midwest was an event of relatively long duration with extreme conditions during its final two days. However, the death toll was about one-fourth the toll for the 1995 heat event in the same region. It seems unlikely that the heat wave death reduction in Chicago is only due to meteorological differences between the two heat waves. An examination shows that both Chicago and St. Louis were quite effective at mitigating their respective heat wave mortality rates (Palecki et al. 2001).

In Europe, according to the annual report of the World Meteorological Organization (Menne 2003), absolute maximum temperature records were exceeded in many areas of France, Germany, the United Kingdom and Switzerland for the first time since the 1940s and/or early 1950s. Beniston (2004) pointed out that 2003 may have been the warmest summer since 1540 according to Pfister et al. (1999). In France alone, about 15,000 people perished (Figure 2).

As one of the fastest growing metropolitan areas in United States, Atlanta, Georgia is often

affected by extreme heat. Most recently, the first 26 days of August, 2007 had high temperatures above 32.2^{o}C, including nine days higher than 37.8^{o}C. The average temperature for this month was 30^{o}C, 3.7^{o}C above normal. The high temperature of 40^{o}C on 23 August was not only the record-breaker for the day, but for the entire month. Kalkstein's research (1993) stated that, under 2^{o}C higher scenario, estimated heat-related death at Atlanta would reach 148 even if people had acclimatized to increased warmth.

Although heat waves have shown obvious impacts on the public's life and property, they seldom provoke a broad federal response. Likewise, most people fail to appreciate the dangers of extreme high temperatures. People who live in cities may be more vulnerable to heat waves because the UHI effect causes a slower cooling process at night, and thus provides little relief from the heat stresses of the day. Considering that an increasing percentage of people will live in cities in coming decades (Figure 3), it is important to continue research characterizing UHI footprints under extreme heat conditions.

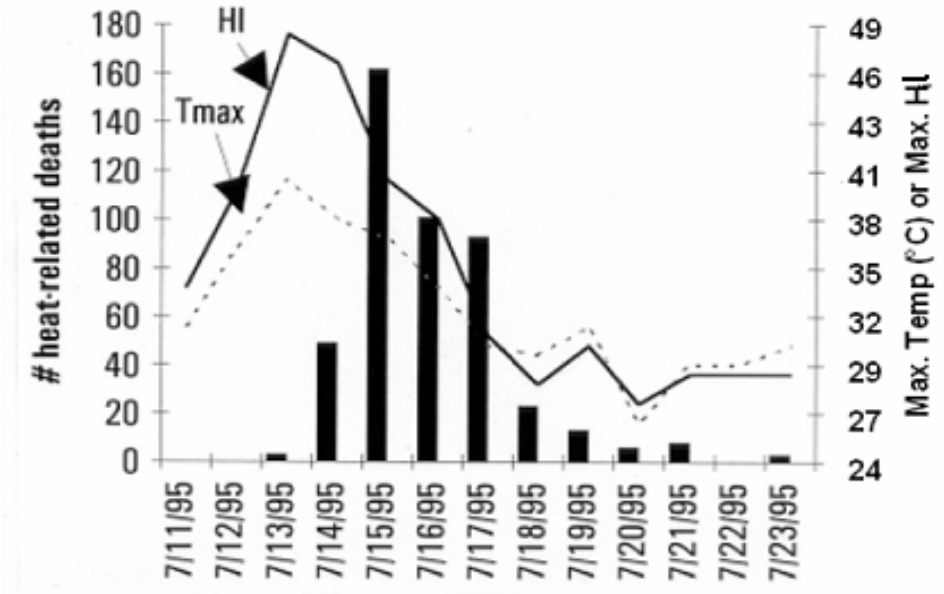

Figure 1 Number of heat-related deaths, maximum temperature (Tmax), and heat index (HI), Chicago, July 11-23, 1995. (Natural disaster survey report: July 1995 heat wave, NWS 1995)

Location	Temperature	Comments
Roth, Germany	40.4C (104.7F)	All time German record high on the 13th
Neutstat, Germany	27.6C (81.7F)	All time overnight high low for Germany
Paris, France	25.5C (77.9F)	All time overnight high low 11th
Turin, Italy	41.7C(107F)	All time record high in 250 years of records on the 11th
Bern, Switzerland	37C(98.6F)	Hottest day since 1865 on the 13th
London (Heathrow), England	37.9C(100.2F)	Hottest observed temperature since records began 130 years ago, on the 11th
Gravesend, England	38.1C(100.6F)	All time England high temperature on the 10th In southeast England.
Badajoz, Spain	44.7C (112.6F)	Highest temperature in 50 years on the 7th

Figure 2 Forecasting Heat Waves using Climatic Anomalies. Data courtesy of the United States Air Force Combat Climatology Center, Ashville, North Carolina.

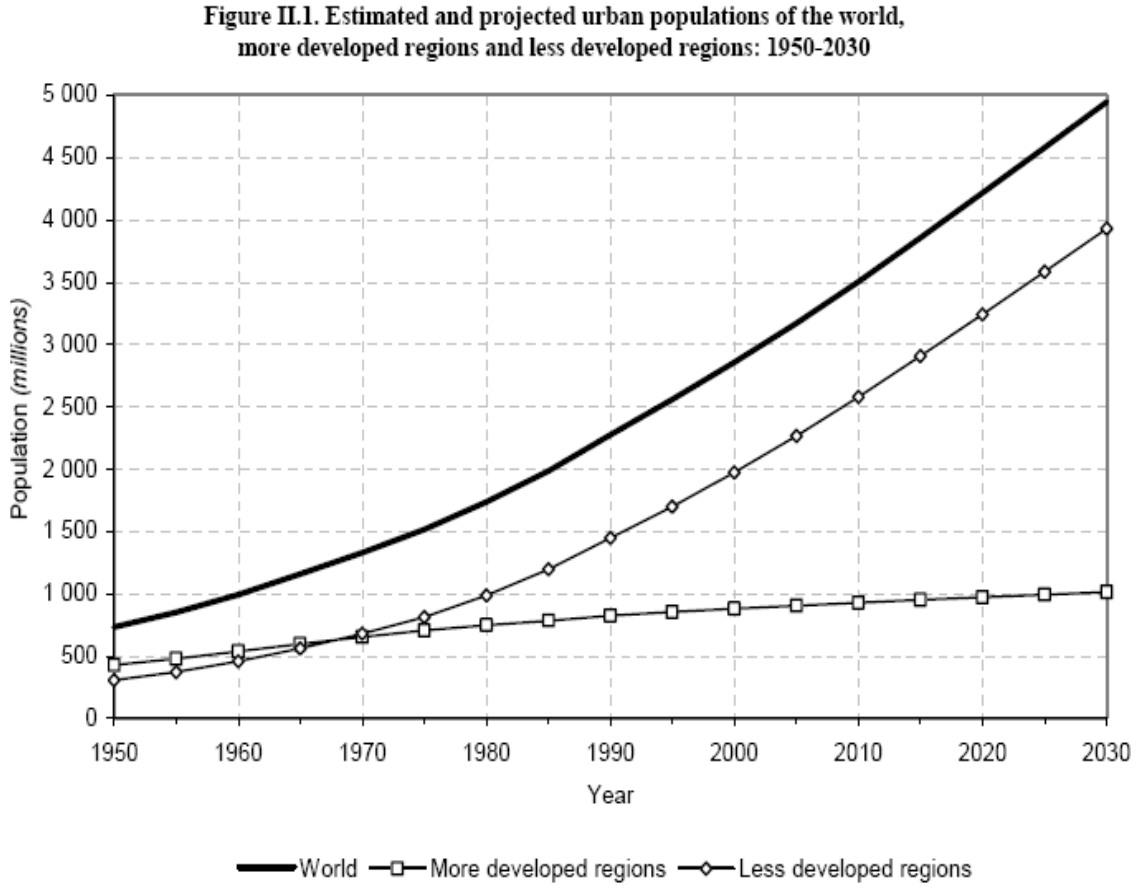

Figure 3 Estimated and projected urban populations of the world, more developed regions and less developed regions: 1950-2030 (United Nations 2004)

1.2 Urban heat island

The unique urban climate has been studied for over 150 years. Howard (1833) was the first to document that urban temperatures were higher than surrounding suburban/rural areas. This phenomenon was called the Urban Heat Island by Manley (1958), and this terminology has been widely used in the literature afterwards. Urban climate summaries by Yoshino (1975), Bornstein and Oke (1980), Oke (1981), Bornstein (1987), Ohashi and Kida (2002), Shepherd et al. (2004), and Bornstein et al. (2006) have shown that under clear skies and light wind conditions, cities are typically warmer than surrounding rural environments by up to 10°C. Brazel et al. 2007 stated that "Recent research summarized by Souch and Grimmond (2006) shows that the UHI (1) is primarily a nocturnal phenomenon, (2) can occur throughout the year, (3) is dependent on weather conditions such as wind and (4) generally consists of higher temperatures in the urban core and commercial locations, with lower temperatures in residential and rural sites."

Heat islands develop in areas that contain a high percentage of non-reflective, impervious surfaces and a low percentage of vegetated and moisture-trapping surfaces. There are several factors that contribute to the formation of the urban heat island. First, heat islands form as a result of urban surfaces materials and structure, such as asphalt, pavement, and roofs, which have low albedos and absorb much of the incoming solar radiation. They re-radiate solar energy in the form of infrared heat. UHI is usually seen at night, when a city will remain warm comparing to surrounding areas even without sun (Taha et al. 1997). Figure 4 shows Atlanta's surface temperature, in which cooler temperatures are yellow and hotter temperatures are red. The urban core is in the center of the images. Second, the lack of urban vegetation such as trees and grass contributes to the heat island effect by reducing evapotranspirational cooling. Third, the urban

heat island is affected by heat exchanges from urban buildings and surfaces. Fourth, human or "anthropogenic" activities act as a heat sources.

In order to understand the mechanism of UHI effects, an introduction to the land surface energy budget is necessary. Urban surface temperature is derived from:

$$(1 - \alpha)\, S\downarrow + LW\downarrow - \varepsilon Tskin^4 - SH - LE - G = 0, \qquad (1)$$

"where SH is sensible heat flux, LW is latent heat flux, and G is the ground heat flux. This equation is the basis of all modern land surface models. SH, LW and G compete for surface net radiation, which is the downward minus upward shortwave and long-wave radiation (the first 4 terms in Eq. (1)). In Eq. (1), α is surface albedo, and S is downward solar radiation, therefore, (1 - α) S↓ is reflected solar radiation. LW↓ is downward long-wave radiation from the surface. Emissivity (ε) and surface skin temperature (Tskin) determine the upward long-wave radiation, or surface emission, following the Stefan-Boltzmann Law. It is evident that urban modifications play important roles on surface temperature changes since the net radiative energy is changed in land surface systems (Jin et al. 2005). In addition, the heights of buildings increase ''roughness length'' and thus SH and LE are affected by enhanced surface turbulence" (Jin et al. 2007).

"Eq. (1) is valid for the natural landscape. While for urban landscapes, there are two additional terms in the surface energy budget: (1) anthropogenic heat flux attributed to fuel combustion, air conditioning, and other human activities (Grimmond; Oke 1999); and (2) storage heat flux due to heat emitted from vertical surfaces such as building walls (Oke 1982)" (Jin et al. 2007).

It is worth noting that although the urban heat island is a well-documented phenomenon, little information is available about heat island characteristics during intensive heat waves such as that in July 1995. Rosenzweig et al. (2005) pointed out that "UHI impacts might be further

amplified during summertime heat wave conditions". According to Kunkel et al. (1996), "the urban heat island at Chicago was pronounced during the 1995 heat wave, and temperature differences were comparable to those found under average summer conditions. Maximum temperature was 1.6°C higher in the city center than in nearby suburban and rural areas, while at night, the difference in minimum temperature was 2 - 2.5 ^{o}C". These findings suggest that forecasts of heat waves for large cities need to carefully consider the abnormal heat island conditions that will exist.

1.3 UHI mitigation strategies

It seems that the increase in temperature to some extent is probably unavoidable due to urbanization; however, there are many steps that may reduce the impacts of heat islands. These steps include (1) installing cool or vegetated green roofs, (2) planting trees and vegetation, and (3) switching to cool paving materials.

Liptan et al. (2004) stated that greening 100% of rooftops in one commercial/industrial neighborhood could reduce that neighborhood's heat island effect by 50-90%, according to the Portland Bureau of Environmental Services. People benefit from installing cool roofs because they can reduce building heat-gain and save summertime air conditioning expenditures. Cool roof materials have two important surface properties: a high albedo and thermal emittance. Taha (1996, 1997) stated that increasing albedo could reduce 1500 LST temperatures in downtown Los Angeles and alter the sea breeze circulation and the mixed boundary layer height thereby improving ozone concentrations. Sailor (1995) used a numerical model to show that "increasing albedo over downtown Los Angeles by 0.14 and over the entire basin by an average of 0.08 decreased peak summertime temperatures by as much as 1.5°C". Sailor et al (2002) explored the

potential of urban heat island mitigation to alleviate heat-related mortality for Philadelphia, PA. Modeling results showed that increasing urban albedo by 0.1 might be responsible for an average daytime air temperature depression of about 0.3 to 0.5 ^{o}C, as well as an overall projected decrease in heat-related mortality.

Planting trees and vegetation may be another effective way to reduce heat islands. Increasing tree cover by 10% (corresponding to about three trees per building) could reduce total heating and cooling energy use by 5 to 10% (McPherson 1994). Vegetation, through latent heat fluxes, cools the air by providing shade and through evapotranspiration. Shaded surface absorbs less amount of solar radiation and thus keeps cool. These cooler surfaces decrease the amount of heat transmitted to buildings and surrounding atmosphere. Vegetation can also cool the air is by absorbing water through their roots and evaporating it through leaf pores. This process uses heat from the air to convert water contained in the vegetation into water vapor. Moreover, this process adds moisture to the air (EPA webpage: Trees and Vegetation).

Cool pavement is also a potential mitigation strategy. Investigations of cool paving materials, although in an early stage, have focused on two mechanisms – surface reflectivity and permeability. Lighter-colored materials have higher solar reflectance, so they absorb less of the sun's energy and stay cooler. Permeable, or porous, pavements allow water to filter into the ground, keeping the pavement cool when moist and can be constructed from a number of materials including concrete, asphalt, and plastic lattice structures filled with soil, gravel, and grass (EPA webpage: What Can Be Done).

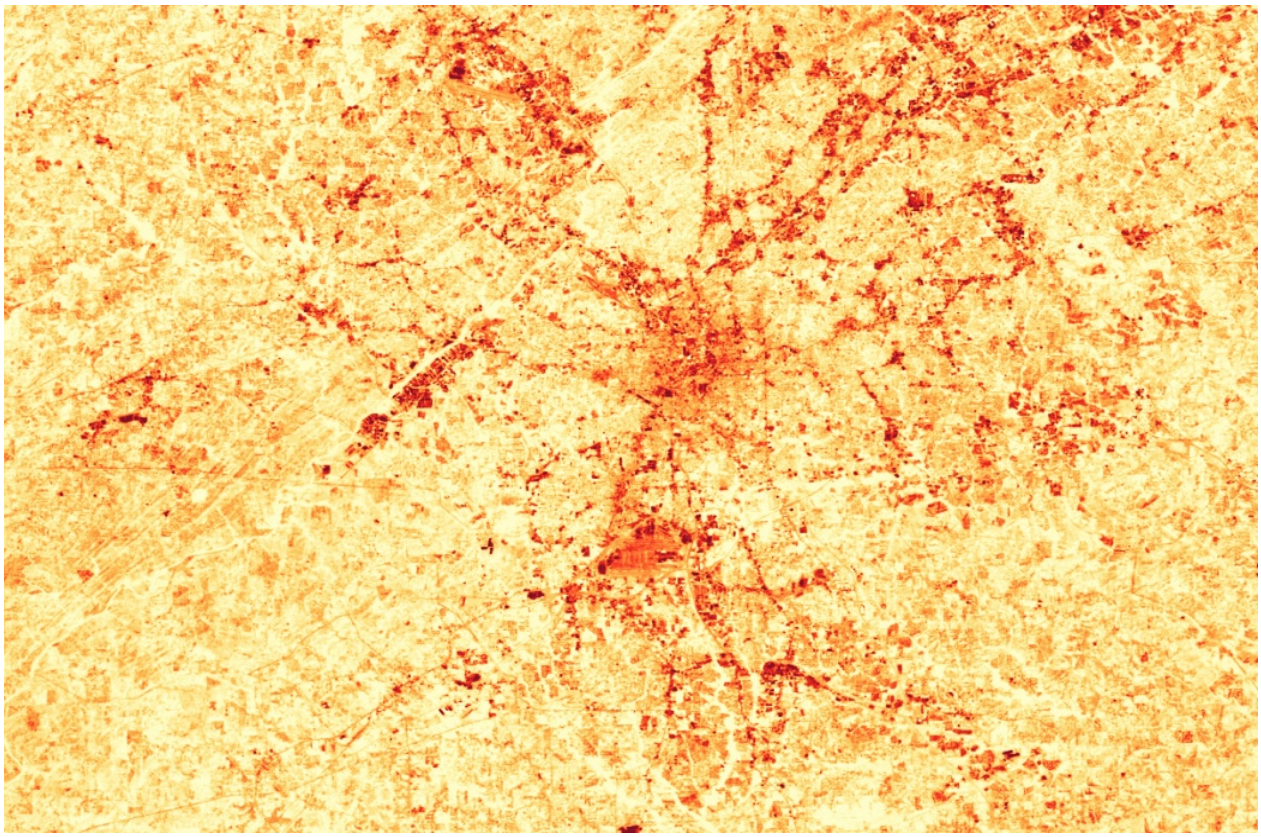

Figure 4 Landsat-7 satellite image of urban Atlanta, Georgia, 20:00 28 September. Deep red colors represent warmest temperatures (courtesy of NASA/MSFC)

CHAPTER 2

Research Questions and Hypotheses

Atlanta is experiencing rapid urbanization and is worthy of further UHI mitigation research. According to Yang and Lo (2003), Atlanta's net increase in urban land from 1999 to 2050 is projected to be 928,379 ha or about 50 ha per day, representing an increase of 254% for the entire period (figure 5). Atlanta was also a part of the Environmental Protection Agency (EPA's) Heat Island Reduction Initiative (HIRI) project. The purpose of this project was to model the impact that widespread heat island mitigation (through albedo and vegetation augmentation) would have on the urban climate of various major US cities. This project's final report (Sailor, 2003) showed that, for Atlanta, a 0.10 albedo increase resulted in an average decrease in maximum air temperature by 0.33°C. Similarly, the average daily maximum temperature was reduced by nearly 0.32°C with a 0.10 vegetation increase. However, it is hard to find this information in the refereed literature, which suggests that more studies of this type are required in Atlanta. Herein, our research seeks to address three research questions.

2.1 What are the seasonal variations in the magnitude of Atlanta's UHI?

The first research objective is to characterize annual and seasonal variations in UHI and quantify its intensity around the metropolitan Atlanta area. The hypothesis is that a statistically-significant positive trend in minimum daily temperature exists for the Atlanta (urban) station as compared to selected rural stations over the last 20-30 years. It is also hypothesized that the

magnitude of the annual UHI has intensified with time while the largest (smallest) UHI magnitude is observed in winter (summer). Surprisingly, It is hard to find any detailed refereed literature study on the climatology of Atlanta's UHI although it has been studied quite often.

2.2 What are the attributes of the Atlanta UHI during extreme heat conditions?

The second aim is to determine Atlanta's UHI intensity under extreme high temperature conditions (i.e., heat waves). Although the UHI effect is detected throughout the year, its occurrence during the summer months is of public policy concern for its potential to be coincident with heat waves. It is hypothesized that UHI magnitude would amplify during heat wave scenarios. This is one of the first studies to examine, from a climatological perspective, Atlanta's UHI under extreme surface temperature conditions.

2.3 What are the first-order effects of proposed mitigation strategies (e.g. albedo surfaces and greening) on UHI intensities?

Thirdly, the Weather Research and Forecast (WRF) model coupled to a land surface model will be employed to simulate metropolitan Atlanta area temperature evolution on a "typical" heat wave day and study how sensitive the UHI is to proposed mitigation strategies (e.g. perturbations to surface albedo and vegetation differences). It is hypothesized that with 100% higher albedo or vegetation fraction alone, the UHI intensity would be mitigated significantly. However, a combination of albedo and vegetation variation may be equally or even more effective. Though not the first study to examine albedo and greening effects, it is one of the first, if not the first, examinations for the Atlanta areas. It may also be the first application of albedo/greening sensitivity experiments to the UHI under extreme heat conditions.

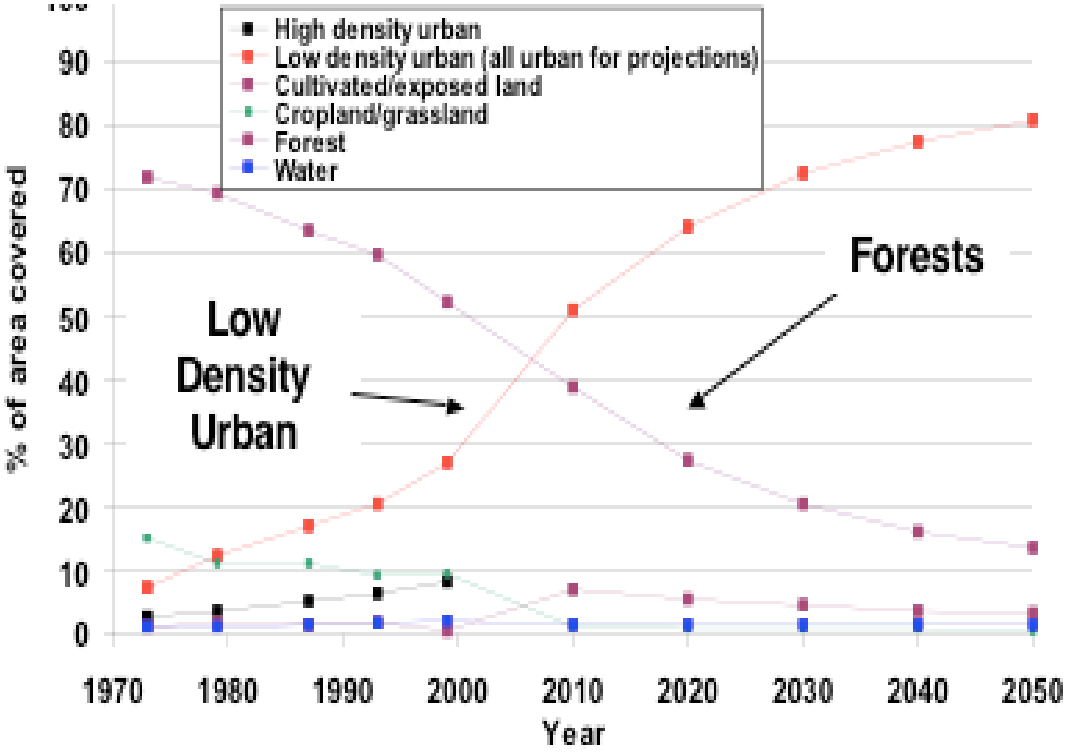

Figure 5 Atlanta urban growth projections (following Yang and Lo 2003).

CHAPTER 3

Methods and Data

3.1 Temperature Analysis Data and Site Selection

The methods utilized in the study consist of statistical analysis and modeling. All of the meteorological data used for statistical analysis were obtained from National Climatic Data Center (NCDC). The data include time series of daily maximum and minimum temperatures for three stations between 1984 and 2007 (except for 1997). This time range was determined by the availability of the data. These stations (see Figure 6) include PDK (located at Atlanta Peachtree Dekalb Airport, GA, representing the "urban" downtown station), AHN (located at Athens Ben Epps Airport, Athens, GA, representing a "hybrid" station), and MONT (located at Monticello, Jasper, GA, representing a "rural" station). Athens was chosen mainly for its development in recent years though it still has attributes of urban and rural sites. Monticello was chosen for its relatively consistent land-use and relative distance from Atlanta. Data for PDK and AHN are derived form Global Summary of The Day (TD-9618), while data for MONT are from Daily Surface Data (TD3200/3210 combined).

The year of 1997 was omitted because PDK had 72% data missing that year. The methods also warranted deleting days with missing data during the other 22 years. After this quality control, the data were 99.1%, 99.8%, and 99.4% complete for PDK, AHN, and MONT respectively.

PDK changed from a Limited Aviation Weather Reporting Station (LAWRS) station to an

Automatic Surface Observing System (ASOS) on 19 March 1998. Athens became ASOS after 1 February 1996 but still serves as a cooperation station. PDK and AHN locations are quite stable, with less than 5m elevation changes during their existence. Monticello remained a cooperative station but experienced elevation changes. Its elevation changed in the following manner: 199.6 m before October 1993, 161.5 m between November 1993 and July 2001, 157.9 m since August 2001. In order to explore the potential effects of this elevation shift on MONT's temperature record, the author checked two other cooperative sites near Monticello. One was Covington in Newton, GA, which experienced a decrease in elevation of approximately 24 m from 1988 to the present. The annual minimum temperature trend for Covington showed a noticeable negative trend similar to Monticello (shown later). Another site was Hawkinsville in Pulaski, GA, which exhibited a slight elevation decrease of approximately 8 m from 1948 to present. No large annual minimum temperature changes were found for Hawkinsville. This result suggests that slight elevation changes may bias the MONT results presented later. However, because there is no stepwise change in the MONT trend and no correlation in the trend-elevation change initiation years; there is confidence in the MONT results. A future study might consider utilizing the Hawkinsville study or a mean of several rural stations. Present research focuses only on the ASOS bias.

Temperature measurement methods are quite different between ASOS and its predecessor: the platinum resistance thermometer (PRT) is used at ASOS and the thermistor sensor at cooperation stations. According to Mckee et. al. (2000), "two questions were raised when ASOS was introduced, (1) What change occurred in the maximum and minimum temperature, and (2) can a climatological average (or 30-year normal) be estimated for the ASOS observations? The questions are related since weather forecasts and verifications, climate monitoring, and

applications all need to know how current observations relate to the past and how they deviate from an average state of climate." ASOS is accurate to $\pm$0.17°C relative to a calibrated field standard instrument. Therefore, it is necessary to carefully explore these changes and differences in order to make sure the constancy and accuracy of temperature data.

In Schrumpf's (1996) research, he determined the temperature difference caused solely by the instrument bias. He pointed out that the seasonal and annual instrument bias values were predominantly negative. Seasonal contribution ranged from -1.21^{o} C (ATL in the fall) to +0.65^{o} C (OHR in the spring). Annual instrument bias ranged from -1.09^{o} C (ATL) to +0.64^{o} C (ORH) (Table 1).

In order to use the above finding, first, it is necessary to calculate the annual average minimum temperature correlation coefficient of the original PDK and AHN data since 1996. The value was 0.67, which indicated a general positive covariance relationship. Next, 1.09^{o} C was added to maximum and minimum temperatures for PDK (after 1998) and AHN (after 1996).

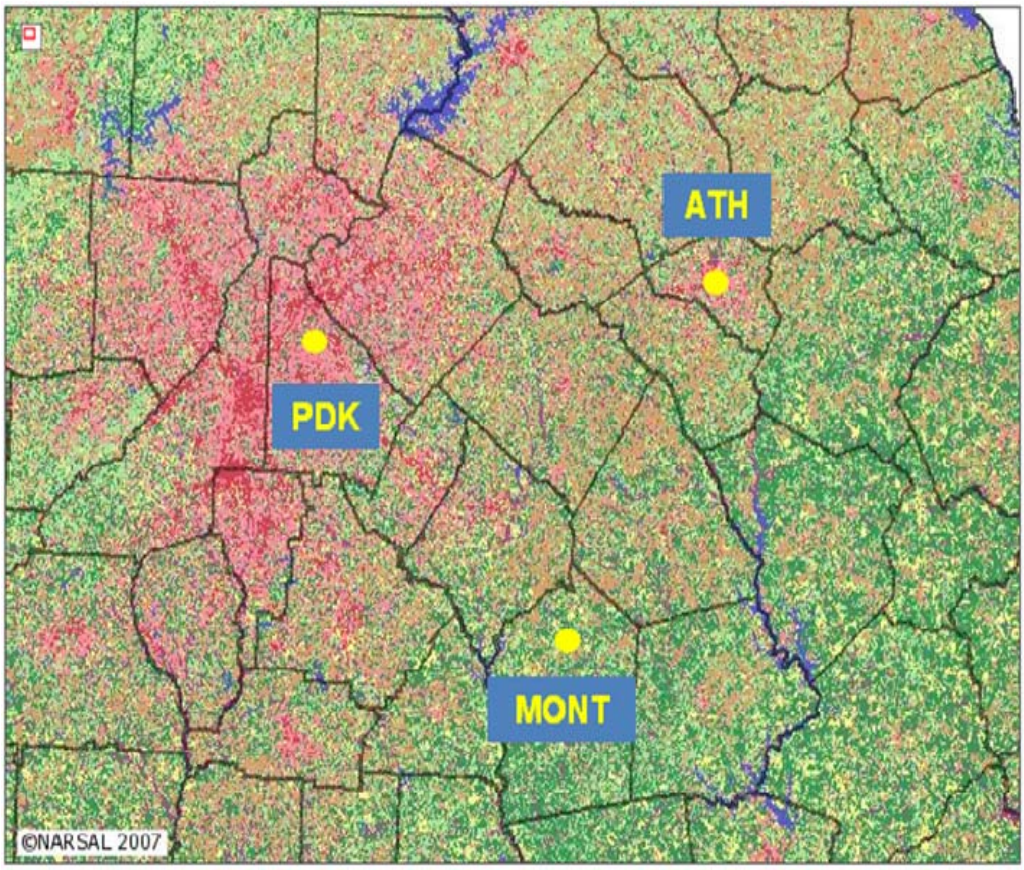

Figure 6 The locations of PDK, AHN, and MONT (courtesy of the University of Georgia School of Ecology, NARSAL).Reddish-pinkish colors represent various levels of "urban" land cover.

Station	Fall Instrument Bias (^{o}C)	Winter Instrument Bias (^{o}C)	Spring Instrument Bias (^{o}C)	Summer Instrument Bias (^{o}C)	Annual Instrument Bias (^{o}C)
ATL	-1.21	-0.99	-1.13	None Given	-1.09

Table 1 Seasonal and annual instrument biases for Atlanta (Schrumpf, 1996).

3.2 Annual and seasonal trend analysis

The annual and seasonal average minimum temperature trends will be examined for the three sites first, followed by UHI effects. The UHI indices are defined as daily minimum temperature differences between PDK-AHN and PDK-MONT. Urban–nonurban differences in minimum temperature serve as the primary indicator of the UHI magnitude because urban–nonurban temperature differences are normally most pronounced at night (Rosenzweig et al. 2005).

Mann-Kendall trend testing (Ezber et al. 2007) will be important for determining the existence and significance of trends. Where appropriate, other statistical tests (e.g. t-tests) will be applied. The nonparametric test of Mann–Kendall is used to determine the existence and significance of a trend in the station data. This method also gives the approximate starting point of a trend and abrupt changes in climate. In the Mann–Kendall method, climate data are enumerated in the time series. For each element y_i , the number n_i of elements y_j preceding it ($i > j$) is calculated in such a way that $y_i > y_j$. The t test statistics is then given by the equation:

$$t = \sum_i n_i$$

and under null hypothesis, t is distributed nearly normal with an expected value and variance;

$$E(t) = \frac{n(n-1)}{4} \text{ and } var(t) = \frac{n(n-1)(2n+5)}{72}$$

When a trend exists, the null hypothesis is rejected for high values of $|u(t)|$ with:

$$u(t) = \frac{[t - E(t)]}{\sqrt{var(t)}}$$

If $u_t > 0$ the trend is positive and if $u_t < 0$ the trend is negative and the significance level is taken to be 95% (±1.96).

The Mann-Kendall test will be employed to analyze (1) minimum temperature trends for PDK, AHN, and MONT, and (2) UHI trends (PDK-AHN, and PDK-MONT). The t-test will be used to verify whether there exist significant differences between UHI values under heat wave days and non-heat wave days.

3.3 Heat wave identification and analysis

Robinson (2000) implied that, "although there had been detailed analyses of individual severe events and their impacts, relatively little was known about the climatic behavior of heat waves. In particular, it was not possible to answer the question, 'Are heat waves changing in severity and frequency?' This failure had direct practical implications for the assessment of the potential impacts of climate change, and a climate description (dataset) was needed to place any particular heat wave in an appropriate historical context. There had been three major factors interacting to impede the development of such a description: the lack of a rigorous definition of a heat wave, the absence of a simple meteorological measure representing the complex interaction between the human body and the thermal environment, and the lack of suitable homogeneous time series for the meteorological variables likely to be involved".

Based on NWS (1994), heat wave was measured by the heat index *Hi*. If diurnal high and nocturnal low heat index values were above the NWS heat stress thresholds (40.7^{o}C and 26.7^{o}C, respectively) for at least two consecutive days, this period can be considered as a heat wave. The heat index combines ambient temperature and humidity, and approximates the environmental aspect a human body, with the NWS thresholds serving as a general estimate of the onset of

physiological stress. However, these thresholds cannot be applied directly nationwide (Robinson, 2000).

To derive a local heat wave definition for Atlanta, present research will follow the methodology similar to Meehl and Tebaldi (2004). Meehl et. al. defined a heat wave based on the concept of exceeding specific thresholds, thus allowing analyses of heat wave duration and frequency. Three criteria were used to define heat waves in this way, which relied on two location-specific thresholds for maximum temperatures. Threshold 1 (T1) was defined as the 97.5th percentile of the distribution of maximum temperatures in the observations and in the simulated present-day climate (seasonal climatology at the given location), and Threshold 2 (T2) was defined as the 81st percentile. A heat wave was then defined as the longest period of consecutive days satisfying the following three conditions: (i) The daily maximum temperature must be above T1 for at least 3 days, (ii) the average daily maximum temperature must be above T1 for the entire period, and (iii) the daily maximum temperature must be above T2 for every day of the entire period. Figure 7 is a schematic illustrating how a heat wave was defined herein.

In this research, the total number of observation days is 8332. T1 is 33.7^{o}C and T2 is 31.1^{o}C. Filtering the maximum temperatures for PDK based on these thresholds and criteria, the heat wave periods are achieved. Table 2 lists the frequency, duration, average maximum temperature, and period of these heat waves. A heat wave did not appear every year. Although the data series began in 1984, there was no heat wave in the first two years. Not surprisingly, all of the heat waves were observed in summer. UHI values between PDK-AHN and PDP-MONT during these heat wave days were calculated and compared with non-heat wave summer days.

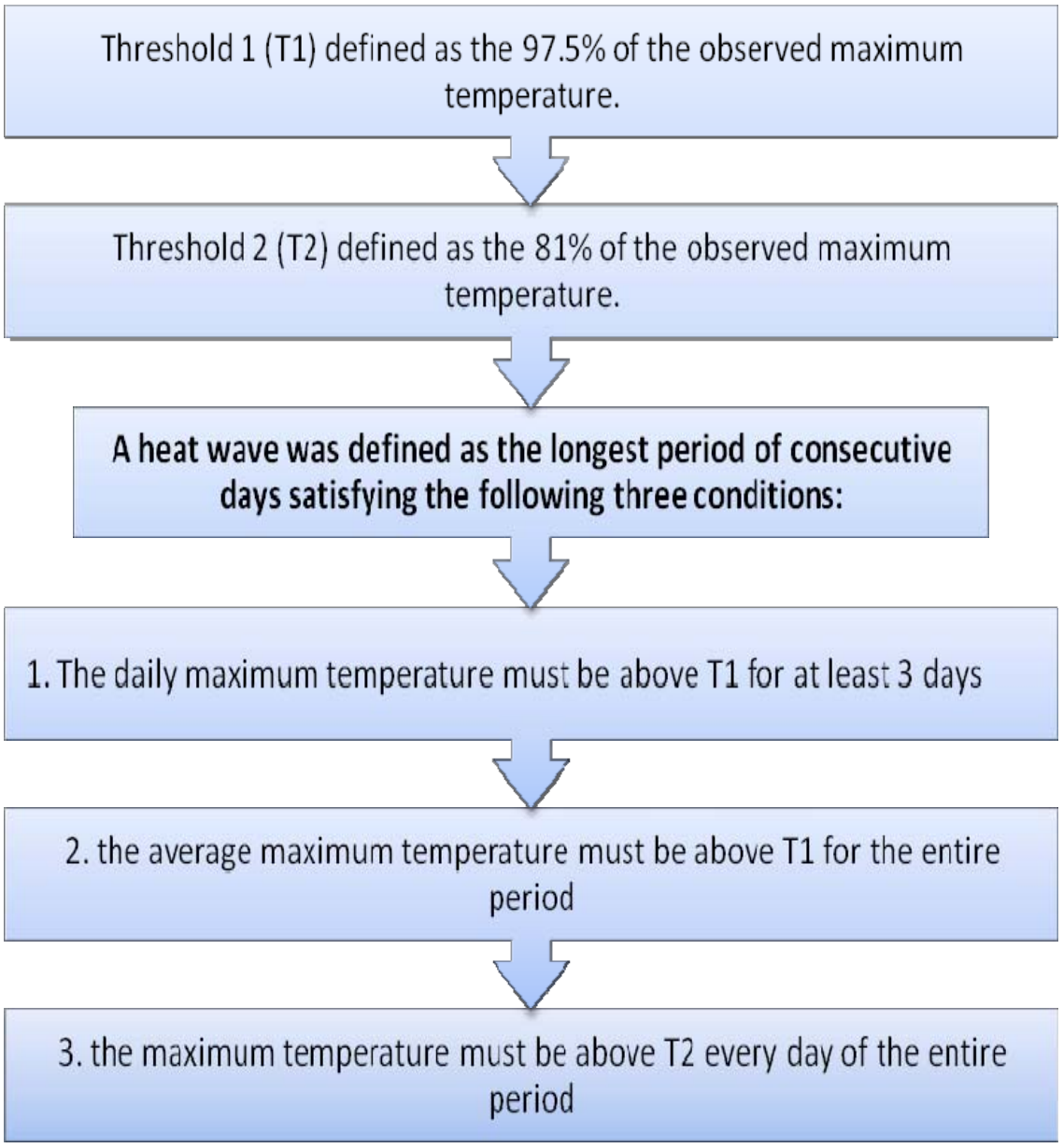

Figure 7 Diagram defining the study's definition of a heat wave.

Year	Frequency	Duration (Unit: day)	Avg. max temperature (^{o}C)	Period (yyyy/mm/dd)
1986	2	4	35.74	19860625 - 19860628
		15	35.60	19860707 - 19860721
1988	1	5	35.79	19880622 - 19880626
1990	1	13	35.61	19900629 - 19900711
1993	1	23	35.61	19930707 - 19930729
1995	2	17	35.59	19950710 - 19950726
		10	37.16	19950810 - 19950819
1998	3	21	35.65	19980621 - 19980711
		7	35.67	19980717 - 19980723
		8	35.61	19980824 - 19980831
1999	1	38	36.46	19990718 – 19990824
2000	2	23	35.82	20000701 - 20000723
		7	36.63	20000814 - 20000820
2002	2	12	35.61	20020727 - 20020807
		9	35.90	20020818 - 20020826
2005	2	8	35.75	20050722 – 20050729
		10	35.56	20050814 – 20050823
2006	3	7	35.67	20060618 – 20060624
		6	35.66	20060630 – 20060705
		33	35.84	20060710 – 20060811
2007	2	5	35.58	20070621 – 20070625
		31	36.27	20070730 – 20070830
Mean	1.83	14.18	35.85	
Std. Dev	0.72	9.89	0.41	

Table 2 List of Atlanta heat waves (1984-2007).

3.4 Numerical model and simulation framework

The Weather Research and Forecasting (WRF) - NOAH Land Surface Model (LSM) is employed in this research to isolate the effects of albedo and vegetation changes on the UHI over the Atlanta region. This coupled WRF-NOAH model can better represent the physical processes such as the exchange and advection of heat, momentum, and water vapor in the urban environment. It can also provide more accurate representation of radiative effects and surface boundary conditions. Traditionally, urban heat island effects have been simulated using three-dimensional mesoscale models linked with standard slab or land surface models, e.g., Sailor 1995, Taha 1997, Haffner and Kidder 1999, Kusaka et al. 2000, Liu et al. 2003. Their results showed that such models were able to capture prominent UHI effects. Therefore, we chose to be consistent with current practice and expertise rather than to employ more simplified approaches.

The WRF model was developed in a collaborative effort by the National Center for Atmospheric Research (NCAR), the National Centers for Environmental Prediction (NCEP), the Forecast Systems Laboratory (FSL), the Air Force Weather Agency (AFWA), Oklahoma University (OU) and other university scientists (Skamarock et al, 2001). It is a non-hydrostatic, compressible, NWP model with mass coordinate system. The basic equations consist of the equations of motion, heat, and moisture, and continuity equation. The Unified Noah-LSM, an advanced land surface/hydrology model, has been recently coupled to the Weather Research and Forecasting (WRF) model (Tewari et al, 2004). It provides surface sensible and latent heat fluxes, and surface skin temperature as lower boundary conditions (Figure 8) for a coupled atmospheric model (Kusaka 2004).

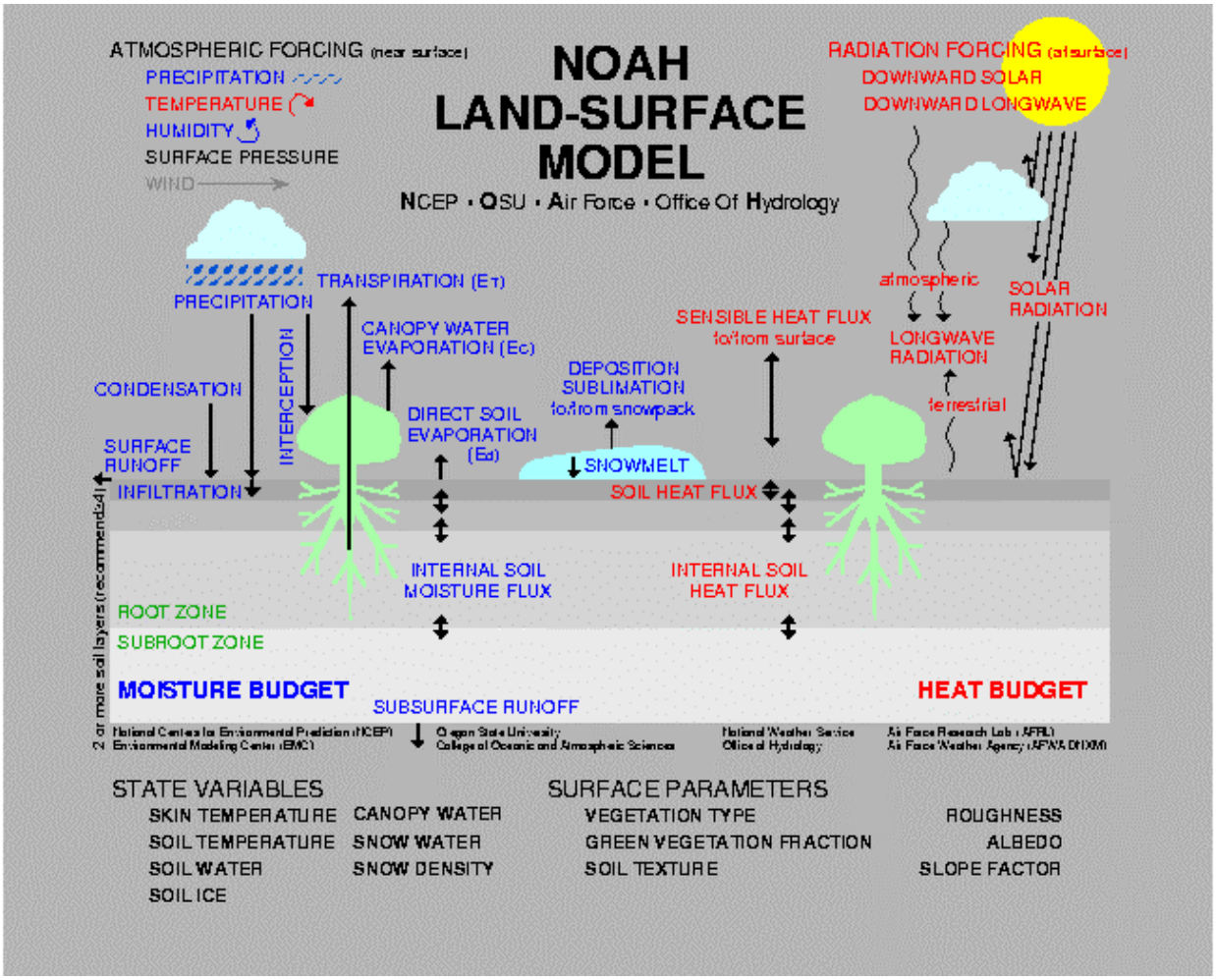

Figure 8 Schematic of the NOAH Land Surface Model (courtesy of UCAR).

In summer, typical albedo for "Urban and Built-up Land" is 15%, 17% for "Dryland Cropland and Pasture", 19% for "Grassland", 12% for "Evergreen Broadleaf /Needleleaf Forest", 16% for "Deciduous Broadleaf Forest", and 14% for "Deciduous Needleleaf Forest", (Table 3 and 4). Typically, the vegetation fraction for land categories is prescribed as a monthly climatological value. However, for the urban areas, "vegetation fraction" will be represented as a function of a parameter called the shade factor (SHDFAC). For the urban land surface, it is initially defined as 0.10. In addition, the radiation stress parameter (RGL) and coefficient for vapor pressure deficit term (HS) will be varied in the same percentage as the shade factor. Both terms can be used as proxies for evapotranspiration in NOAH. RGL and HS are inversely proportional to evapotranspiration, so they would be decreased with larger SHDFAC.

It should be noted that due to model limitations, urban land cover as opposed to detail urban land use, will be considered to investigate hypothetical response of the UHI to my sensitivity analysis. Future studies should exploit the emerging generation of high resolution urban canopy models. However, there is still a lack of detailed urban morphological parameters for Atlanta.

Methodologically, the first step is to select a case study from the recent heat waves of 2007. The aforementioned discussion suggested that there were two heat wave events in 2007, one from 21 to 25 June, and the other from 30 July to 30 August. During the two heat wave periods, the largest UHI magnitudes were detected on 16 August 2007, for both PDK-AHN (3.28 ^{o}C) and PDK-MONT (6.61 ^{o}C). The case run time starts at 0000 UTC, 16 August (2000 EDT, 15 August) through 1200 UTC 17 August (0800 EDT, 17 August).

Figure 9 shows the 3-nested grid configuration of this modeling framework. The resolutions are 18km, 6km and 2km, respectively, with the highest resolution grid centered over Atlanta. Figure 10 shows detailed land cover for the inner-most domain.

USGS 33,2, SUMMER	ALBD	SLMO	SFEM	SFZ0 T	HERIN	SCFX	SFHC
1,	15.,	.10,	.88,	80.,	3.,	1.67,	18.9e5,'Urban and Built-Up Land'
2,	17.,	.30,	.985,	15.,	4.,	2.71,	25.0e5,'Dryland Cropland and Pasture'
3,	18.,	.50,	.985,	10.,	4.,	2.20,	25.0e5,'Irrigated Cropland and Pasture'
4,	18.,	.25,	.985,	15.,	4.,	2.56,	25.0e5,'Mixed Dryland/Irrigated Cropland and Pasture'
5,	18.,	.25,	.98,	14.,	4.,	2.56,	25.0e5,'Cropland/Grassland Mosaic'
6,	16.,	.35,	.985,	20.,	4.,	3.19,	25.0e5,'Cropland/Woodland Mosaic'
7,	19.,	.15,	.96,	12.,	3.,	2.37,	20.8e5,'Grassland'
8,	22.,	.10,	.93,	5.,	3.,	1.56,	20.8e5,'Shrubland'
9,	20.,	.15,	.95,	6.,	3.,	2.14,	20.8e5,'Mixed Shrubland/Grassland'
10,	20.,	.15,	.92,	15.,	3.,	2.00,	25.0e5,'Savanna'
11,	16.,	.30,	.93,	50.,	4.,	2.63,	25.0e5,'Deciduous Broadleaf Forest'
12,	14.,	.30,	.94,	50.,	4.,	2.86,	25.0e5,'Deciduous Needleleaf Forest'
13,	12.,	.50,	.95,	50.,	5.,	1.67,	29.2e5,'Evergreen Broadleaf Forest'
14,	12.,	.30,	.95,	50.,	4.,	3.33,	29.2e5,'Evergreen Needleleaf Forest'
15,	13.,	.30,	.97,	50.,	4.,	2.11,	41.8e5,'Mixed Forest'
16,	8.,	1.0,	.98,	0.01,	6.,	0.,	9.0e25,'Water Bodies'
17,	14.,	.60,	.95,	20.,	6.,	1.50,	29.2e5,'Herbaceous Wetland'
18,	14.,	.35,	.95,	40.,	5.,	1.14,	41.8e5,'Wooded Wetland'
19,	25.,	.02,	.90,	1.,	2.,	0.81,	12.0e5,'Barren or Sparsely Vegetated'
20,	15.,	.50,	.92,	10.,	5.,	2.87,	9.0e25,'Herbaceous Tundra'
21,	15.,	.50,	.93,	30.,	5.,	2.67,	9.0e25,'Wooded Tundra'
22,	15.,	.50,	.92,	15.,	5.,	2.67,	9.0e25,'Mixed Tundra'
23,	25.,	.02,	.90,	10.,	2.,	1.60,	12.0e5,'Bare Ground Tundra'
24,	55.,	.95,	.95,	5.,	5.,	0.,	9.0e25,'Snow or Ice'
25,	30.,	.40,	.90,	1.,	5.,	.62,	12.0E5,'Playa'
26,	18.,	.50,	.95,	15.,	6.,	.62,	12.0E5,'Lava'
27,	70.,	.40,	.90,	1.,	5.,	0.,	12.0E5,'White Sand'
28,	15.,	.02,	.88,	80.,	3.,	1.67,	18.9e5,'Unassigned'
29,	15.,	.02,	.88,	80.,	3.,	1.67,	18.9e5,'Unassigned'
30,	15.,	.10,	.88,	80.,	3.,	1.67,	18.9e5,'Unassigned'
31,	10.,	.10,	.97,	80.,	3.,	1.67,	18.9e5,'Low Intensity Residential '
32,	10.,	.10,	.97,	80.,	3.,	1.67,	18.9e5,'High Intensity Residential'
33,	10.,	.10,	.97,	80.,	3.,	1.67,	18.9e5,'Industrial or Commercial'

Table 3 The standard USGS landuse table employed in the WRF model. ALBD (albedo).

Vegetation Parameters
USGS

27,1,	'ALBEDO	Z0	SHDFAC	NROOT	RS	RGL	HS	SNUP	LAI	MAXALB'	
1,	.15,	1.00,	.10,	1,	200.,	999.,	999.0,	0.04,	4.0,	40.,	'Urban and Built-Up Land'
2,	.19,	.07,	.80,	3,	40.,	100.,	36.25,	0.04,	4.0,	64.,	'Dryland Cropland and Pasture'
3,	.15,	.07,	.80,	3,	40.,	100.,	36.25,	0.04,	4.0,	64.,	'Irrigated Cropland and Pasture'
4,	.17,	.07,	.80,	3,	40.,	100.,	36.25,	0.04,	4.0,	64.,	'Mixed Dryland/Irrigated Cropland and Pasture'
5,	.19,	.07,	.80,	3,	40.,	100.,	36.25,	0.04,	4.0,	64.,	'Cropland/Grassland Mosaic'
6,	.19,	.15,	.80,	3,	70.,	65.,	44.14,	0.04,	4.0,	60.,	'Cropland/Woodland Mosaic'
7,	.19,	.08,	.80,	3,	40.,	100.,	36.35,	0.04,	4.0,	64.,	'Grassland'
8,	.25,	.03,	.70,	3,	300.,	100.,	42.00,	0.03,	4.0,	69.,	'Shrubland'
9,	.23,	.05,	.70,	3,	170.,	100.,	39.18,	0.035,	4.0,	67.,	'Mixed Shrubland/Grassland'
10,	.20,	.86,	.50,	3,	70.,	65.,	54.53,	0.04,	4.0,	45.,	'Savanna'
11,	.12,	.80,	.80,	4,	100.,	30.,	54.53,	0.08,	4.0,	58.,	'Deciduous Broadleaf Forest'
12,	.11,	.85,	.70,	4,	150.,	30.,	47.35,	0.08,	4.0,	54.,	'Deciduous Needleleaf Forest'
13,	.11,	2.65,	.95,	4,	150.,	30.,	41.69,	0.08,	4.0,	32.,	'Evergreen Broadleaf Forest'
14,	.10,	1.09,	.70,	4,	125.,	30.,	47.35,	0.08,	4.0,	52.,	'Evergreen Needleleaf Forest'
15,	.12,	.80,	.80,	4,	125.,	30.,	51.93,	0.08,	4.0,	53.,	'Mixed Forest'
16,	.19,	.001,	.00,	0,	100.,	30.,	51.75,	0.01,	4.0,	70.,	'Water Bodies'
17,	.12,	.04,	.60,	2,	40.,	100.,	60.00,	0.01,	4.0,	35.,	'Herbaceous Wetland'
18,	.12,	.05,	.60,	2,	100.,	30.,	51.93,	0.02,	4.0,	30.,	'Wooded Wetland'
19,	.12,	.01,	.01,	1,	999.,	999.,	999.0,	0.02,	4.0,	69.,	'Barren or Sparsely Vegetated'
20,	.16,	.04,	.60,	3,	150.,	100.,	42.00,	0.025,	4.0,	58.,	'Herbaceous Tundra'
21,	.16,	.06,	.60,	3,	150.,	100.,	42.00,	0.025,	4.0,	55.,	'Wooded Tundra'
22,	.16,	.05,	.60,	3,	150.,	100.,	42.00,	0.025,	4.0,	55.,	'Mixed Tundra'
23,	.17,	.03,	.30,	2,	200.,	100.,	42.00,	0.02,	4.0,	65.,	'Bare Ground Tundra'
24,	.70,	.001,	.00,	1,	999.,	999.,	999.0,	0.02,	4.0,	75.,	'Snow or Ice'
25,	.30,	.01,	.50,	1,	40.,	100.,	36.25,	0.02,	4.0,	69.,	'Playa'
26,	.16,	.15,	.00,	0,	999.,	999.,	999.0,	0.02,	4.0,	69.,	'Lava'
27,	.60,	.01,	.00,	0,	999.,	999.,	999.0,	0.02,	4.0,	69.,	'White Sand'

Table 4 The standard USGS vegetation parameter table employed in the WRF model. Parameters that determine evapotranspiration are RGL (radiation stress) and HS (vapor pressure deficit).

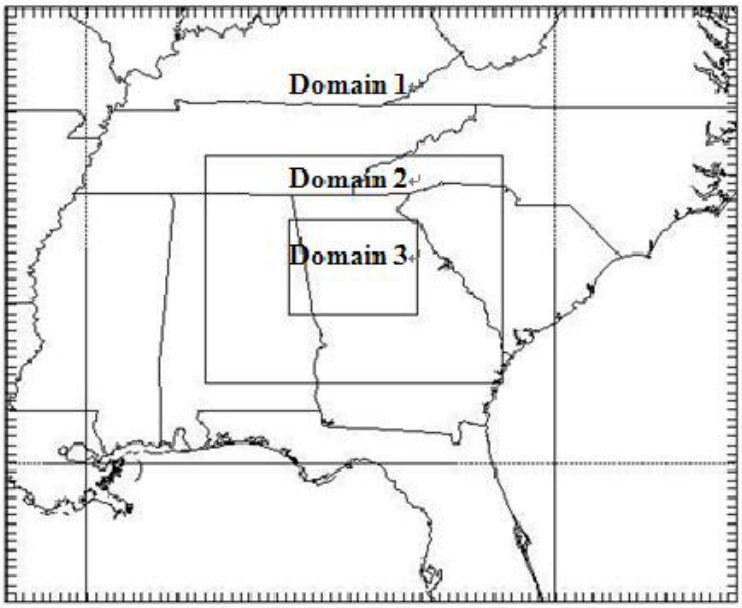

Figure 9 WRF 3-nested grid configuration

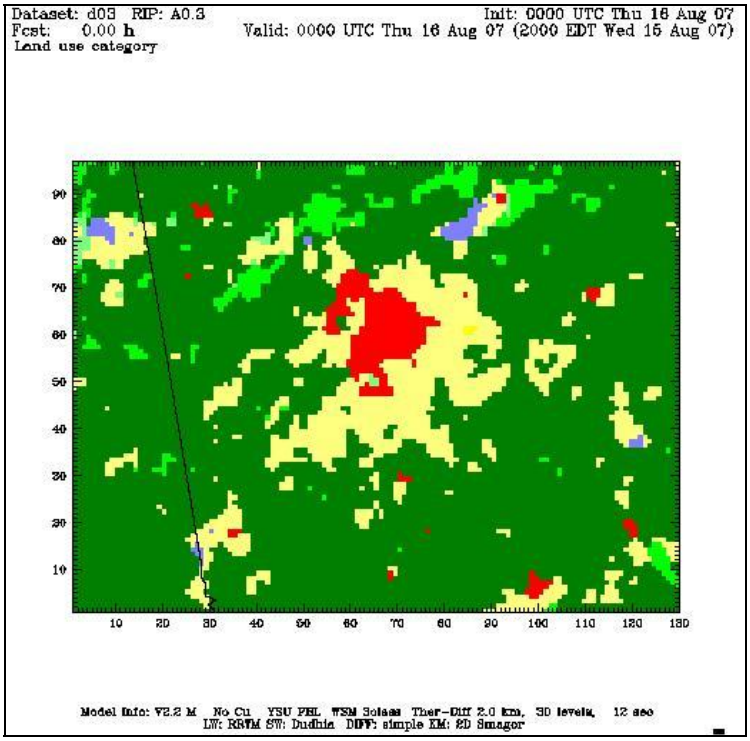

Figure 10 Land cover for Domain 3. The colors represent the following: red-"urban and built up land", yellow-"dryland cropland and pasture", light and dark green-"vegetation and forest", and blue-"water body".

Initialization data were obtained from North American Regional Reanalysis (NARR). NARR data covers the period from 1979 to near-real time. It contains fully cycled 3-hour Eta Data Assimilation System, with the highest resolution, 32km horizontally and 45 levels. This data provides radiosonde-detected temperature, winds, and humidity, and surface-observed pressure, as well as other data from satellites. Output from the model experiments includes hourly 2-m shelter temperature, latent flux, and upward surface (sensible) heat flux. It should be noted that, as Taha (1999) discussed, 2-m shelter height temperature is a common measure of the UHI but represents a second-order response of surface fluxes to changes in skin-temperature. Both temperature and fluxes will be explored although only 2-m shelter height data is readily available for validation.

The second step is to test UHI sensitivity to albedo and vegetation fraction values (e.g. SHDFAC and associated evapotranspiration) to simulate, theoretically, proposed mitigation strategies. Specifically, albedo values for "urban and build-up land" in LANDUSE.TBL and VEGPARM.TBL will be changed, from its original 0.15 to desired values. The parameters SHDFAC (shade factor), RGL (radiation stress) and HS (vapor pressure deficit) can be found and changed in VEGPARM.TBL. As aforementioned, RGL and HS vary by the same percentage to represent evapotranspiration. For the scope of this project, only simplified experiments are conducted to understand how Atlanta's UHI under extreme heat responds to the mitigations strategies. A more detailed research project should be applied to ascertain more rigorous results.

An ensemble of sensitivity experiments will be conducted, and the parameter values are listed in Table 5.

CONTROL - Standard run initialized with North American Regional Reanalysis data

NOURBAN – replace the urban area with cropland parameters

ALBEDO - Increase urban albedo value by 100%

GREEN- Increase SHDFAC, and evapotranspiration by 100%

ALBEDO+GREEN- Increase urban albedo, SHDFAC, and evapotranspiration by 100%

In case there is no marked difference between sensitivity and control scenarios, we will increase the albedo and/or vegetation fraction gradually. The primary output includes spatio-temporal variation of 2-m temperature and flux variables. It should be noted that by no means do these experiments represent the full ensemble of experiments that can be conducted. This project was interested in first order effects. More detailed study and modeling is required in the future.

	Albedo	SHDFAC	RGL	HS
CONTROL	0.15	0.1	999	999
NOURBAN	0.19	0.8	100	36.25
ALBEDO	0.30	0.1	999	999
GREEN	0.15	0.2	499.5	499.5
ALBEDO+GREEN	0.30	0.2	499.5	499.5

Table 5 Parameter values in five model scenarios.

CHAPTER 4

Results

4.1 Surface-observed minimum temperature patterns and trends

The minimum temperature yearly trends are calculated for PDK, AHN, and MONT. In Figure 11, the annual minimum temperatures are represented as a line chart. The minimum temperature trend for PDK was expected to have a more significant increasing trend compared with that for AHN and MONT.

A peculiar temperature peak exists in 1998 for the three sites. One possible explanation is the data calibration. In order to correct ASOS bias, 1.09^{o} C was added to PDK since 1998 and to AHN since 1996. A more likely explanation is the omission of the 1997 data since the data calibration would not explain the peak in the MONT data.

The 1998 minimum temperature is replaced by the averaged 1996 and 1999 values. After smoothing the anomaly, linear trend lines are added to each site, Figure 12, 13, and 14, PDK show a slight negative and nearly flat trend, about -0.23^{o} C per decade. Minimum temperature at AHN increased substantially, 0.70^{o} C per decade. At MONT, a negative trend was observed, -1.79^{o} C per decade.

Table 6 shows the p-values for the three sites from the Mann-Kendall test. The p-value for PDK is 0.1015. If assuming $P<0.05$ as standard, the negative trend at PDK was not statistically significant. While at AHN and MONT, the p-values are 0.0003 and 0.0001, respectively, which means there is 99.3% (99.9%) chance that the positive (negative) trends at AHN (MONT) are

real. This result is reasonable. PDK was urban through much of the period of study so its minimum temperature did not change very much and always reflected a UHI bias. Athens probably was in the process of slight urbanization, so its minimum temperature increased in response thereby increasing its minimum temperature. Monticello probably stayed rural. However, MONT's decreased elevation may contribute to its negative minimum temperature trend. The elevation effect may be questionable since the starting points for the cooling trends are not coincident with the aforementioned years when elevation changed at MONT. There is also no stepwise change when elevation changed. Overall, the above findings are contrary to the originally hypothesis but expected in light of the discussion.

Mean monthly minimum temperatures for PDK, AHN, and MONT within the research period (1984 to 2007, except 1997) are plotted as line charts (Figure 15). Patterns for the three sites are similar, with hottest months in summer (June, July, and August) and coldest months in winter (Dec, Jan, and Feb). Minimum temperature for PDK is always the maximum, and MONT is always the minimum. In summer months, all of the values for PDK are above 20^{o} C. The average UHI magnitide for PDK-AHN and PDK-MONT is 1.31^{o} C and 1.71^{o} C, respectively. This result provides a fairly conclusive picture of the relative magnitude of Atlanta's UHI. Results from case study modeling days by Haffner and Kidder (1999) and Taha (1999) suggest that the mean UHI can range from 0.8 to 2.5^{o} C in Atlanta, which is consistent with our climatological findings.

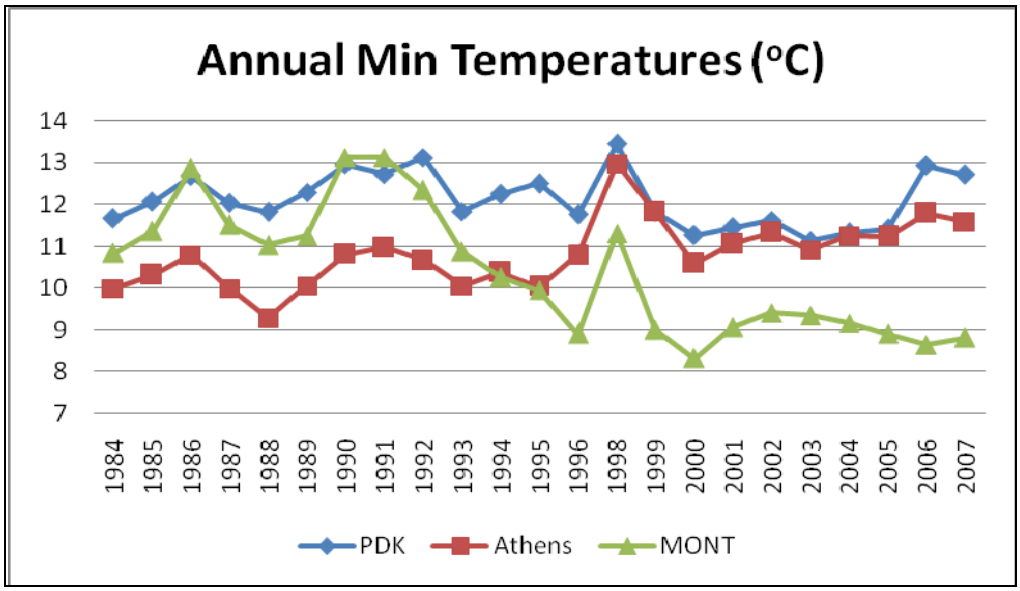

Figure 11 Annual minimum temperatures at PDK, Athens, and Monticello

(Units: Degree Celsius)

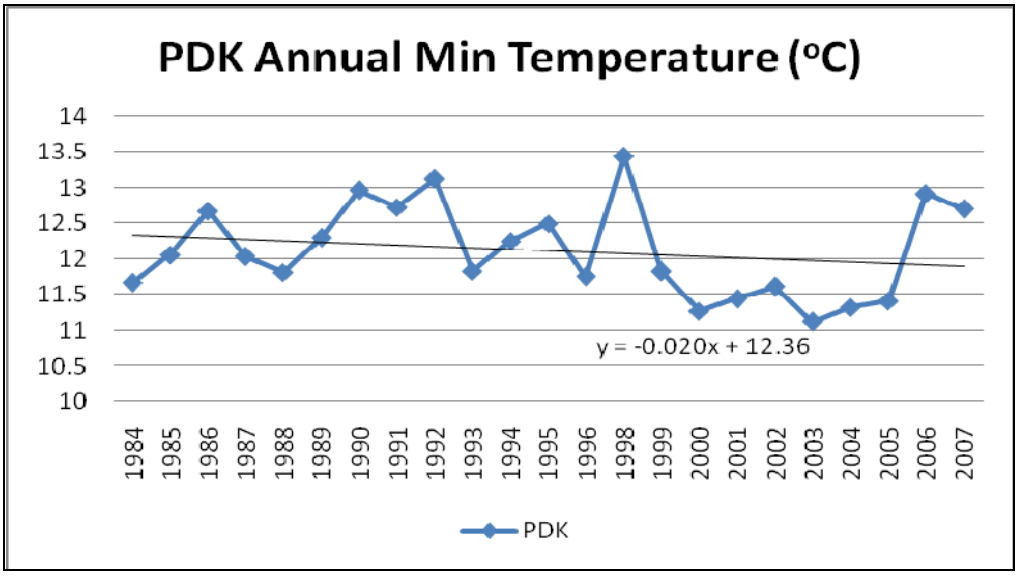

Figure 12 Annual minimum temperature and trend line at PDK (Units: Degree Celsius)

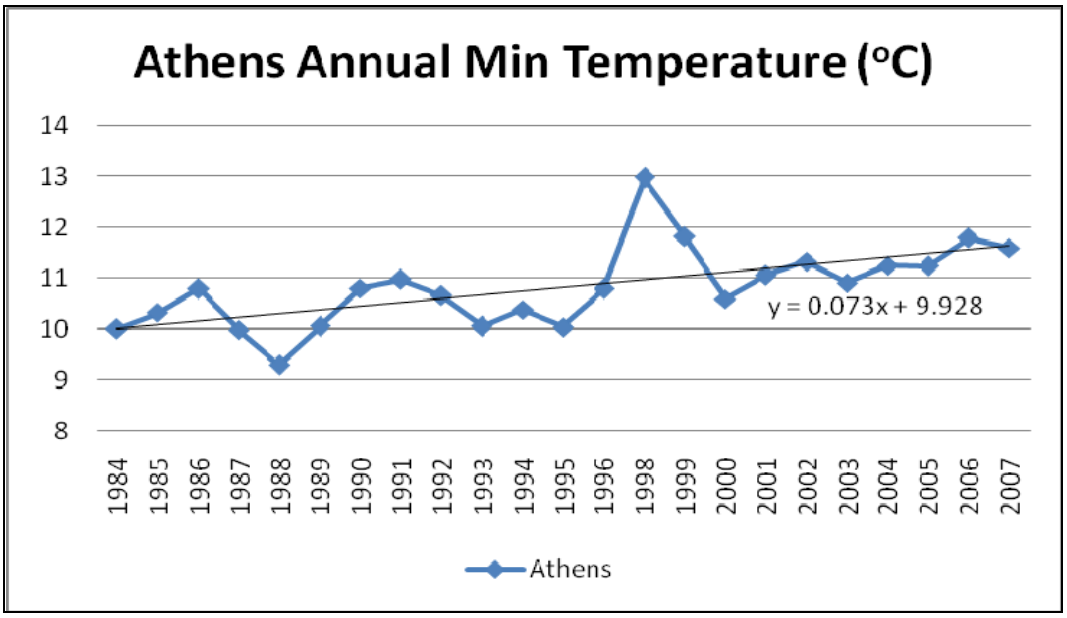

Figure 13 Annual minimum temperature and trend line at Athens (Units: Degree Celsius)

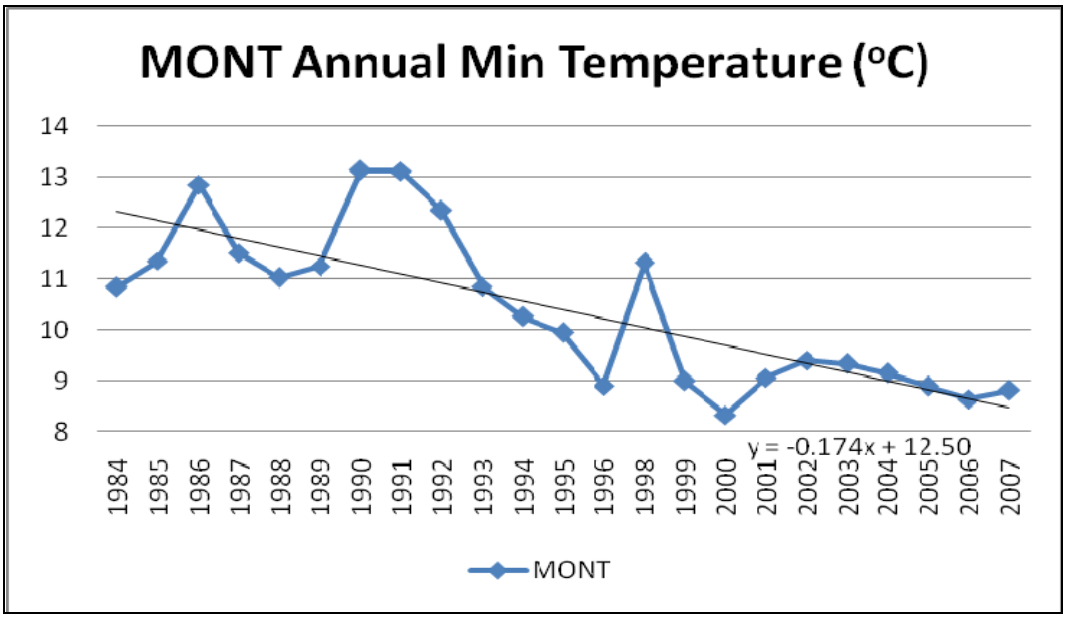

Figure 14 Annual minimum temperature and trend line at Monticello (Units: Degree Celsius)

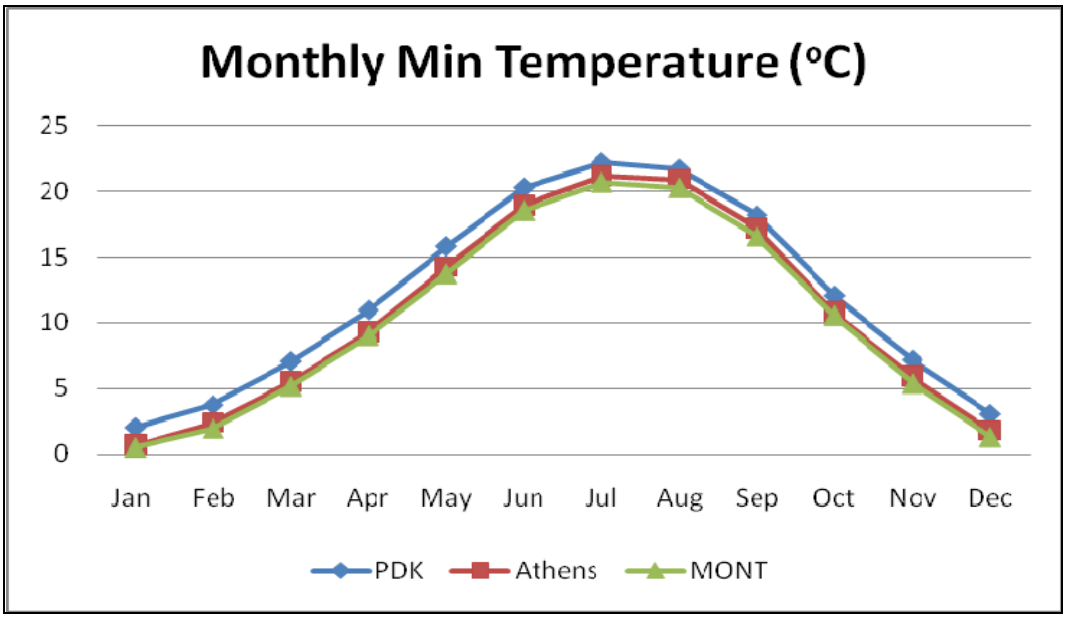

Figure 15 Monthly minimum temperatures at PDK, AHN, and MONT (Units: Degree Celsius)

Mann-Kendall test	PDK	AHN	MONT
Trend (^{o}C per decade)	-0.23	0.70	-1.79
P-value	0.1015	0.0003	0.0001

Table 6 P-values of annual minimum temperature trends for three sites from Mann-Kendall testing.

4.2 Surface-observed UHI patterns and trends

The annual UHI trends are calculated for PDK-AHN and PDK-MONT. In Figure 16, the annual UHIs are represented as a line chart. It was expected that magnitude of the annual UHI has intensified with time. However, there were changes around 1996 for both PDK-AHN and PDK-MONT. Before 1996, the PDK-AHN UHI magnitude exceeded the PDK-MONT UHI consistently. After 1996, PDK-AHN UHI decreased and PDK-MONT increased. The implementation of ASOS at PDK and AHN may have caused such changes. Another possible explanation is the steady urbanization at Atlanta and Athens decreased the UHI magnitude relative to the consistently rural Monticello site. Yet, a third explanation is that cooling related to elevation changes caused this shift. But as noted earlier, the year 1996 is not consistent with when elevation changes occurred.

In order to clarify the UHI trends, the research period is separated into two sections, 1984 to 1995 and 1996 to 2007. Then the Mann-Kendall tests are applied for both sections and the whole study period (1984-2007). The results are shown in Table 7. If $p < 0.05$, the trend can be considered as significant. However, in any separated section, p-values are bigger than 0.05. This result indicates that, no significant UHI trend existed in either period before or after 1996. Even though the data has been calibrated since 1996, the data continuity problem is still not clearly understood. For the entire period, PDK-AHN UHI has a significant decreasing trend (p-value equal to 0.0022 and -0.87^{o} C per decade) and PDK-MONT has a significant increasing trend (p=value equal to zero and 1.45^{o} C per decade).

The monthly UHI magnitude was expected to the largest in winter and the smallest in summer. However, in Figure 17, it is worthy of notice that the largest UHIs were in spring. For PDK-AHN, April has a peak UHI value of 3^{o} C. For PDK-MONT, May has peak UHI value, of

3.7^{o} C. For both PDK-AHN and PDK-MONT, the smallest UHIs exist in summer, with minimum values in August, 1.43^{o} C and 2.6^{o}C, respectively. The seasonal UHI pattern may be affected by seasonal cloudiness around Atlanta. Figure 18 illustrates the cloud fraction for a 1° x 1° box centered over Atlanta. Approximately 8 years of cloud fraction data (Ignatov et al. 2005) from the MODIS instrument (daytime data from the Terra spacecraft and nocturnal data from Aqua spacecraft) was acquired from the NASA data archive center at Goddard Space Flight Center. Daytime clouds have a direct impact on incoming short wave radiation, and thus on the surface energy budget. It is expected that more clouds indicate lower surface temperature and less absorption of shortwave energy. Figure 18 shows that the daytime cloud fraction was indeed high in summer months of July and August, which might explain why the UHI is at a minimum. Further, the figure also reveals a relative minimum in daytime cloud fraction during the spring period that may explain the UHI peak. Although other factors could certainly be occurring.

The finding of a weaker UHI in summer is consistent with Kim and Baik (2002)'s investigation of Seoul, Korea's UHI although, they found stronger UHI's in the winter and fall rather than spring. However, they did note that the trend in UHI over a 24 year period was greatest during the spring. The emergence of spring vegetation may result in a larger albedo gradient with the urban area, which would cause a larger UHI. According to Unger et al (2001), the seasonal UHI pattern may be determined to a high degree by urban surface factors, and cloudiness and wind speed may play a negative role on the development of UHI. Liu et al (2007) stated that the seasonal UHI variation tended to be negatively correlated with the seasonal variation of relative humidity and vapor pressure.

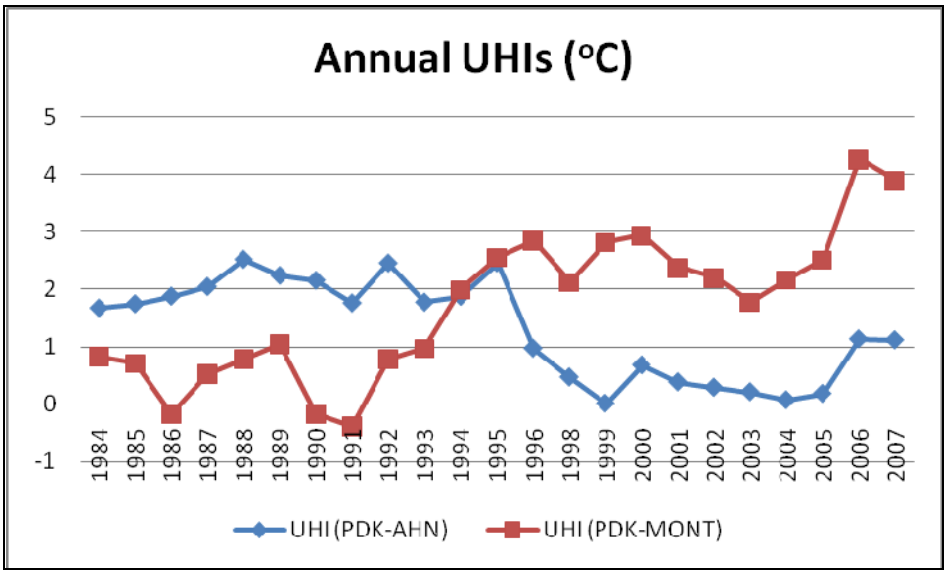

Figure 16 Annual UHIs, PDK-ATH and PDK-MONT (Units: Degree Celsius)

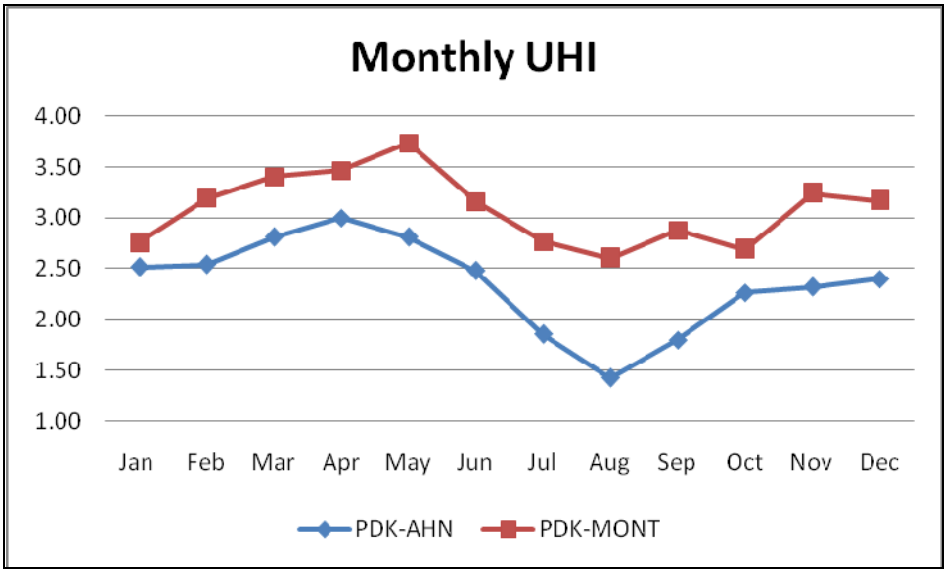

Figure 17 Monthly UHI intensities (Units: Degree Celsius)

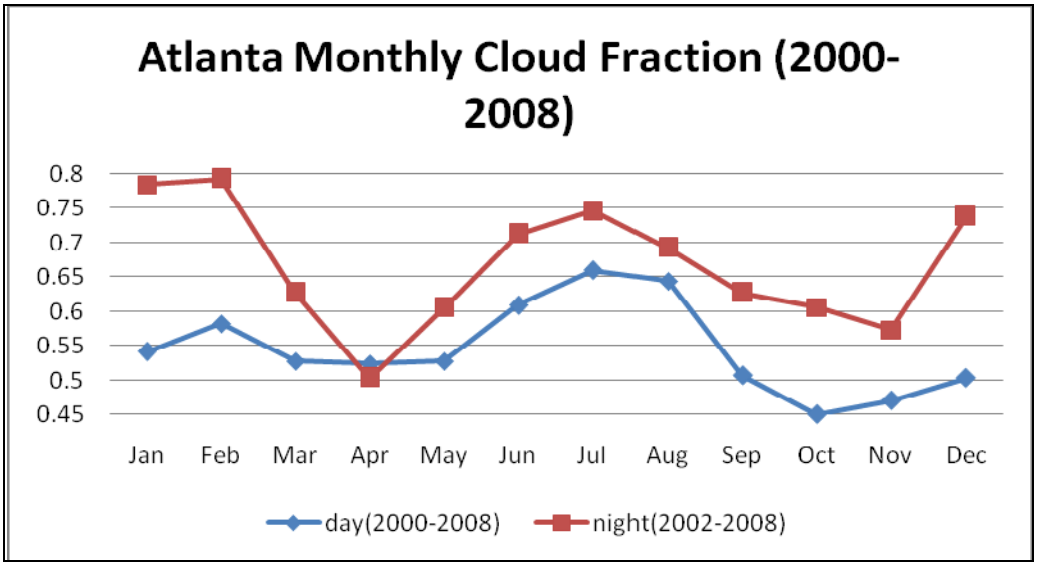

Figure 18 Atlanta Monthly Cloud Fraction (2000-2008). Data is provided by the MODIS cloud fraction product from the Terra and Aqua spacecrafts (NASA-GSFC).

Annual UHI P-value	1984-1995	1996-2007	1984-2007
PDK-AHN	0.2437	0.8763	0.0022
PDK-MONT	0.1148	0.4363	0.0000

Table 7 P-values of UHI trends for PDK-AHN, and PDK-MONT from Mann-Kendall testing.

4.3 Heat wave frequency and strength trends

The UHI values during heat wave and non-heat wave days in summer are listed in table 8. During the period 1984-2007, a heat wave in Atlanta occurred during 50% of the years. Atlanta heat waves occurred exclusively in the summer months. The mean number of heat waves events in Atlanta during a given heat wave year was 1.83. The results also revealed that, on average, Atlanta heat waves lasted 14.18 days although there was quite a bit of variability (standard deviation of 9.89). The mean maximum temperature during Atlanta's heat waves was 35.85° C.

It is expected that UHI magnitude would be larger in heat wave days. Unpaired and unequal t-tests are employed to investigate whether the UHI differences under these two conditions are significant. For the PDK-AHN UHI, the t-test reveals that t = -0.8783 and P-value = 0.1901 when hypothesizing that the UHI during heat waves was smaller. For the PDK-MONT UHI, the t-test result is t = 10.7637 and P-value = 0 when hypothesizing that the UHI during heat waves was large. This result implies that, for PDK-AHN, the UHI magnitude difference between heat wave days and non-heat wave days is not significant. While for PDK-MONT, the UHI magnitude in heat wave days is virtually 100% certain to be larger than non-heat wave days.

UHI (^{o} C)	Heat wave days	Non-HW Summer days	t-value	p-value
PDK-AHN	0.99	1.08	-0.8783	0.1901
PDK-MONT	2.43	1.42	10.7637	0

Table 8 UHI differences between heat wave and non-heat wave days.

4.4 WRF modeling outputs

- **2-m shelter height temperature spatial distribution**

There are five scenarios to simulate 2-m shelter height temperature around the Atlanta metropolis. For CONTROL, no parameter is different from the standard USGS land cover and vegetation parameter tables. The output from CONTROL can be used as background. Any other scenarios would be compared with CONTROL.

Figures shown below are the 2m shelter height temperature maps at 1400 EDT for all of the five scenarios. The time 1400 EDT was selected because the UHI phenomena was of greatest magnitude for this extreme heat case day according to observations. It is somewhat surprising to find an afternoon UHI peak at Atlanta because the literature often discusses peak UHI several hours after sunset, at midnight, or early morning. However, daytime UHIs are not uncommon. In fact, Haffner and Kidder (1999) noted that during their simulation, a daytime UHI also existed in one of their case days. Their Case 2 day showed that the daytime UHI is the result of the soil and sensible heat flux differences. During the day all three surface-related fluxes (soil, sensible, and latent heat flux) can be important depending on the situation. In relatively dry urban conditions, the latent heat flux difference is also significant during the daytime. Taha's (1999) simulations for Atlanta resolved a daytime heat island on the order of 2.5° C around 1400 LST. His high albedo simulations reduced the UHI by 0.5 to 1.0° C (due to reduction in SSH Flux). It should be noted that this was not an extreme heat day case.

It is important to note that the model performed very well in capturing the realistic temperature evolution on this day. Further, although the UHI peak was in the afternoon, the model does capture a fairly significant UHI in the overnight-early morning hours when it is expected, climatologically.

For CONTROL, the heat island became visible at 1000 EDT and lasted through 1400 EDT, 16 August. Meanwhile, there was a thermal low pressure centered north-northeast of Atlanta. This low is likely triggered by temperature gradient between Atlanta and its surrounding areas and may have implications for why previous work has resolved a rainfall anomaly in that region (see Mote et al. 2007 for references). The red color indicates relatively higher temperature, and blue indicates relatively cooler temperatures (Figure 19).

For NOURBAN, the city of Atlanta is removed and replaced by the dominant land cover type of the surrounding rural location, i.e., 'dryland, cropland and pasture'. The urban area was replaced by cropland (Figure 20). After removing the urban area, noticeable changes can be observed (Figure 21). Figure 21 shows the T2 difference between CONTROL and NOURBAN. Over Atlanta at 1400 EDT, the 2-m temperature for NOURBAN is 2 to 3° cooler.

For ALBEDO, when urban albedo increased 100%, there was no dramatic difference from CONTROL (Figure 22). This indicates that increasing albedo by 100% was not an effective mitigation strategy for lowering Atlanta's 2-m height temperature. If urban albedo is tripled from 0.15 to 0.45, the highest T2 at 1400 EDT over Atlanta drops approximately 2.5° C and the thermal low disappears (Figure 23). It is worth noting that the triple albedo scenario looks similar to NOURBAN. This may imply that although several parameters can influence T2, large albedo changes have a strong impact. It is fair to question whether a realistic strategy for increasing Atlanta's albedo by a factor of three could ever be a chief. This suggests that a combination of mitigation strategies may be more feasible.

For GREEN, the highest T2 in the urban area drops to 306 K (32.9^{o} C). Atlanta is about 7° cooler in this scenario than CONTROL (Figure 24). The larger shade factor and evapotranspiration can increase latent heat and reduce surface sensible heat, which may explain

why T2 decreases dramatically. This is also encouraging because doubling vegetation in Atlanta might be a more feasible approach than tripling the albedo.

For ALBEDO+GREEN, the T2 pattern is quite similar to CONTROL but 1 K (1^{o} C) cooler. The thermal low is also present (Figure 25). This finding is consistent with Sailor (1995) and others who have found that a combined albedo and greening strategy is not necessarily more effective than the individual mitigation strategies alone.

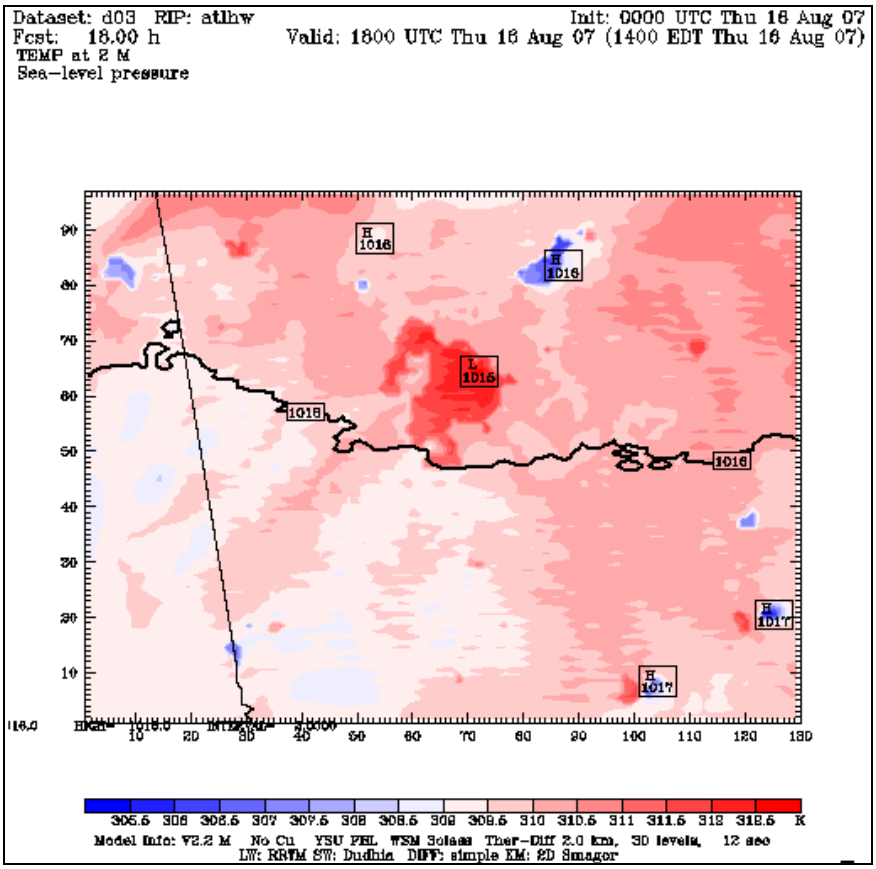

Figure 19 2-m shelter height temperature for CONTROL, 1400 EDT, 16 August 2007

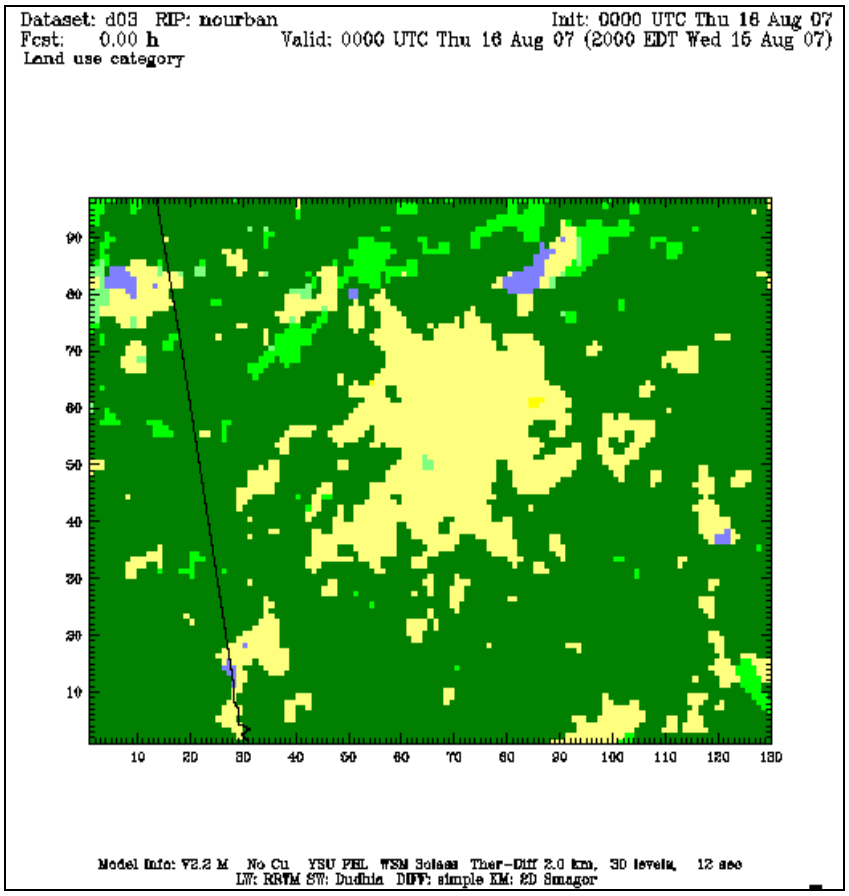

Figure 20 Land cover for Domain 3, same as Figure 10 but with urban land cover replaced with drylanc/cropland.

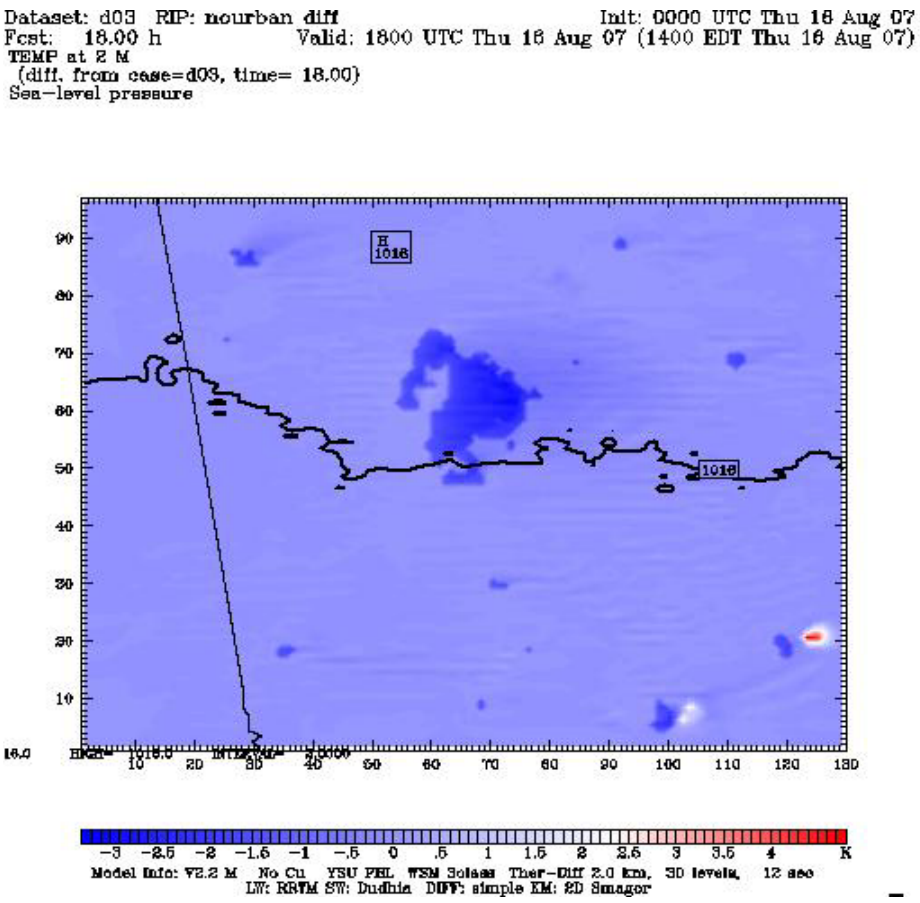

Figure 21 NOURBAN 2m shelter height temperature difference

from CONTROL at 1400 EDT 16 August 2007

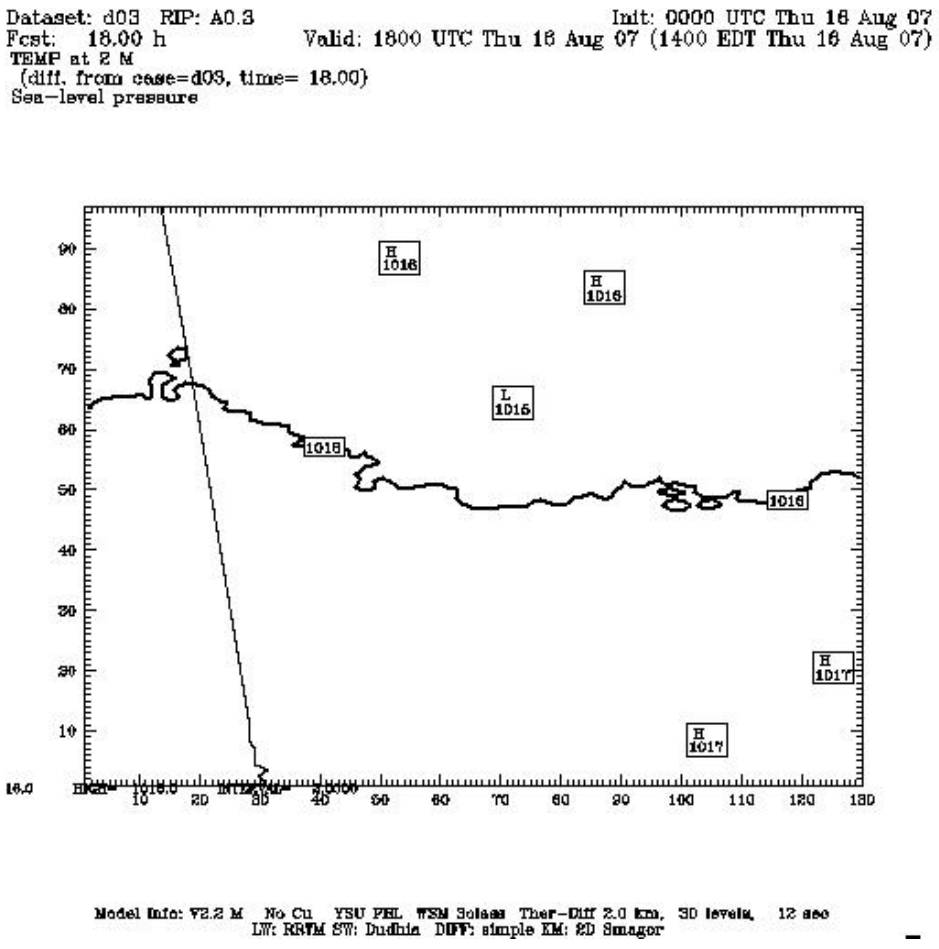

Figure 22 ALBEDO 2m shelter height temperature difference from CONTROL at 1400 EDT 16 August 2007

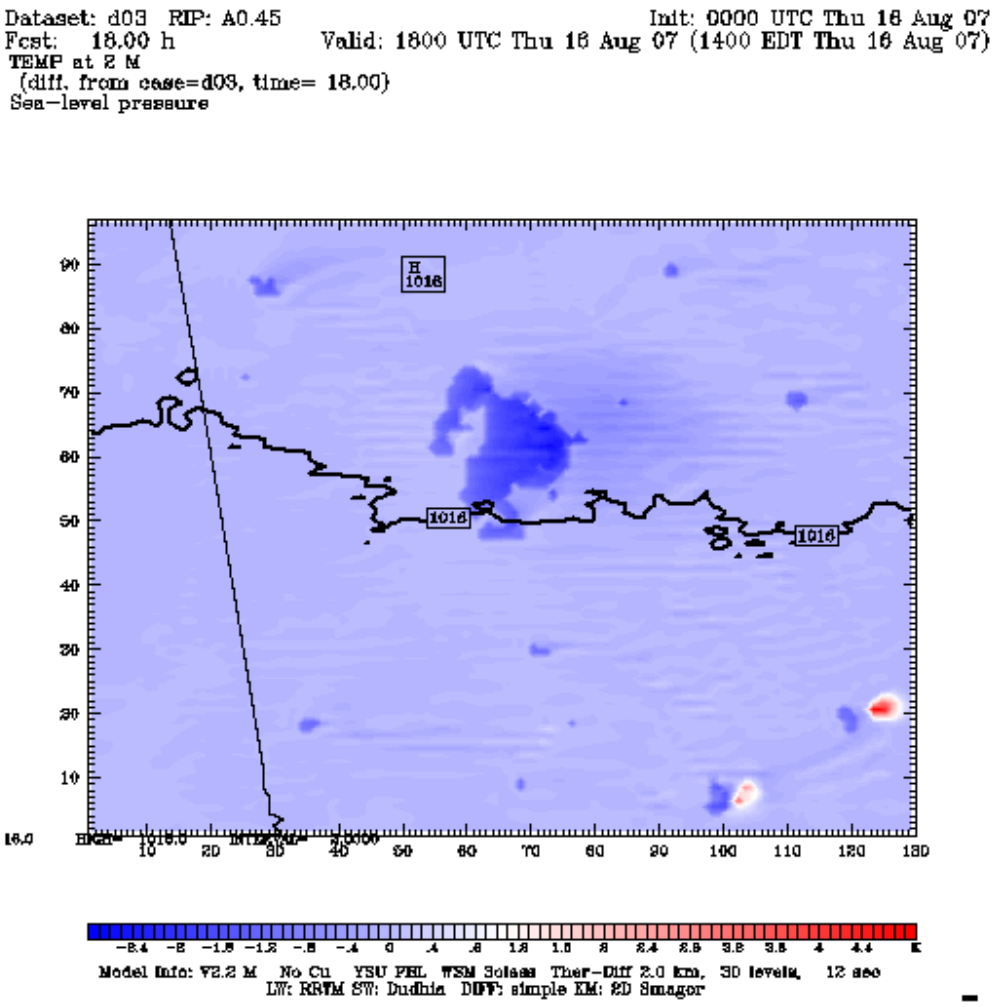

Figure 23 3x ALBEDO 2m shelter height temperature difference from CONTROL at 1400 EDT 16 August 2007

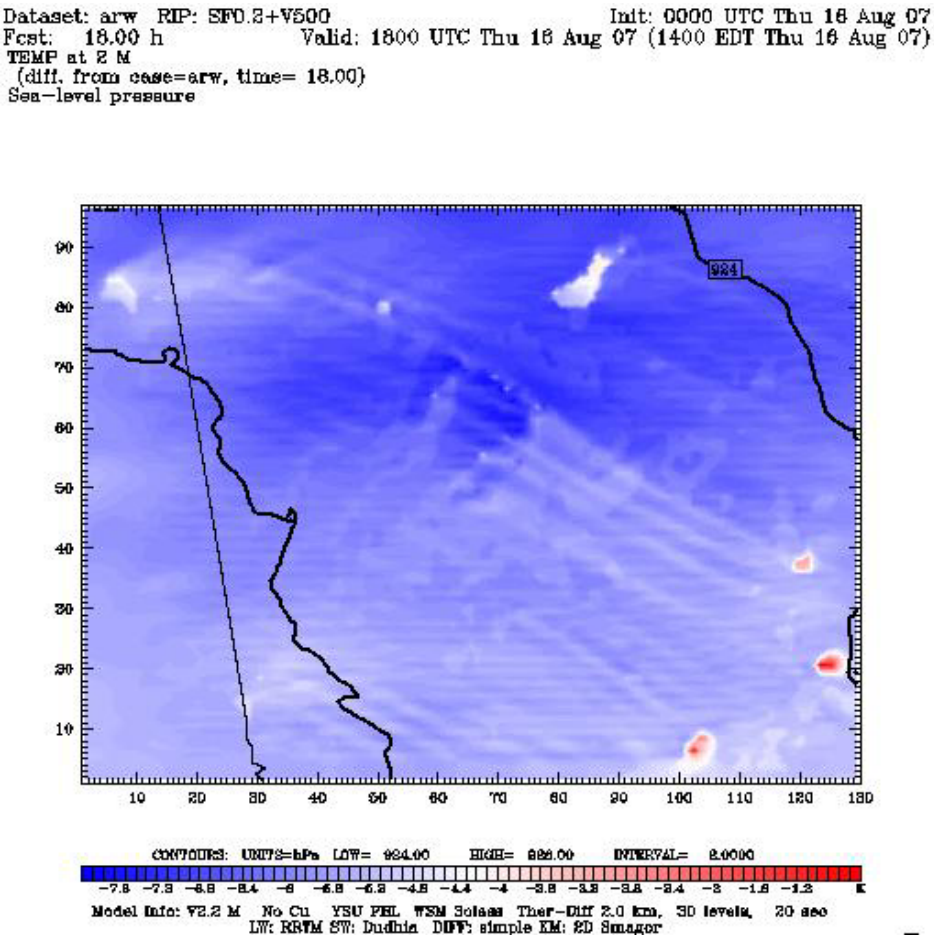

Figure 24 GREEN 2m shelter height temperature difference from CONTROL at 1400 EDT 16 August 2007

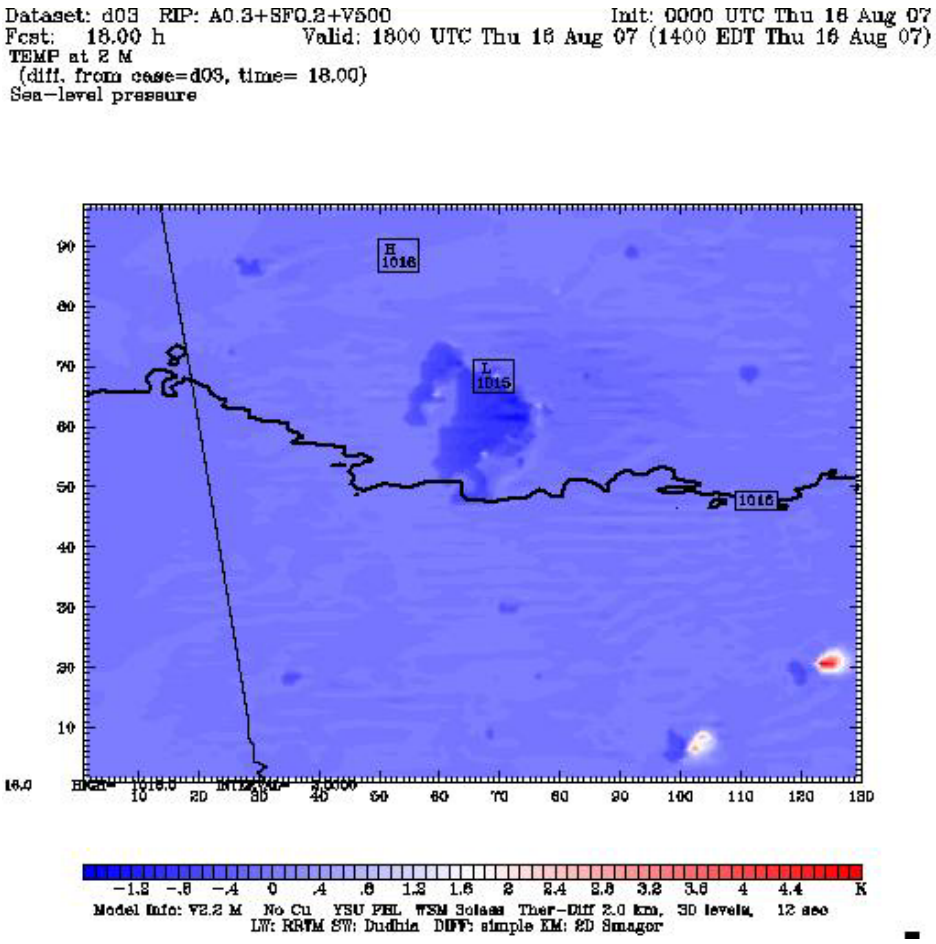

Figure 25 ALBEDO+GREEN 2m shelter height temperature difference from CONTROL at 1400 EDT 16 August 2007

- **2-m shelter height temperature and fluxes temporal distribution**

Three points (PDK, AHN, and MONT) are selected from WRF Domain 3. For PDK, four time series are plotted (e.g. 2m shelter height temperature (T2), latent heat flux (LH), upward heat flux at the surface (HFX), and downward short wave flux at ground surface (SWDOWN). The PDK-AHN and PDK-MONT UHIs are plotted in a manner similar to the observational analysis presented earlier. Latent heat flux is related to evapotranspiration, and upward heat flux represents sensible heat, which is caused, in part, by stored heat in the urban canopy or anthropogenic heat discharge. SWDOWN determines how much solar radiation energy the ground surface can achieve and is equal to zero at night. The total forecast time is 36 hours (from 2000 EDT, 15 August to 0800 EDT, 17 August 2007).

Figure 26 shows the time series for T2. One interesting result is that T2 at 1500 EDT 16 August drops sharply for CONTROL, while other scenarios have a relatively smooth change. However, no such phenomenon was recorded after checking the hourly temperature data of PDK that day. According to the hourly data, temperatures at 1400 and 1500 were both 311 K (37.9^{o}C) (see Figure 27). The CONTROL simulation is likely producing some clouds at this time (possibly urban-induced). Figure 27 also provided quantitative evidence that the model is capturing the real heat island evolution nicely on this particular case day.

Comparing these five scenarios, GREEN is most effective at reducing T2. At 1400, T2 for GREEN is 7^{o} C lower than CONTROL. T2 is 2.5^{o} C lower for NOURBAN and unchanged 0^{o} C ALBEDO. T2 is 0.9^{o} C lower for the hybrid simulation of ALBEDO+GREEN. Taha (1999)'s high albedo simulations reduced the Atlanta UHI by 0.5 to 1.0° C (due to reduction in surface sensible heat flux). It should be noted that his case was not an extreme heat day. Also, Sailor

(1995) found that increasing albedo over downtown Los Angeles by 0.14 and over the entire basin by an average of 0.08 decreased peak summertime temperatures by as much as 1.5° C.

Figure 28 and 29 show the 2-m height temperature UHIs of PDK-AHN and PDK-MONT: (1) For PDK-AHN, CONTROL and ALBEDO overlap. In these two scenarios, the UHI peaks at noon, while still present through midnight. The sharp decrease indicates the influence of the cloud cooling discussed earlier. The UHI in GREEN peaks at 1400 EDT and is still present late into the evening (0400 EDT). The UHI ALBEDO+GREEN peaks at 2200 EDT, while its daytime UHI is also marked. NOURBAN shows an urban cold island (UCI) at most times. (2) For PDK-MONT, CONTROL and ALBEDO have the same UHI values. GREEN has a relatively small UHI magnitude in the daytime. NOURBAN still shows UCI at most times of the day. The UHI for CONTROL, ALBEDO, NOURBAN, and ALBEDO+GREEN peak around 2200 EDT, while for GREEN, it peaks at noon. Except for NOURBAN, a daytime and nocturnal UHI is captured by the model. Based on this modeling result, it may be more appropriate to define UHI by using urban/nourban minimum temperature differences for PDK-MONT. This would also be consistent with the observational analysis that suggested that the magnitude of the PDK-MONT UHI was larger.

Figure 30 plots the time series for LH. It implies that latent heat fluxes are close to zero at night and early morning and begin to increase at 0800. LH peaks in the afternoon, around 1400-1500 and then diminishes to near zero at 2000. This happens because latent heat relates closely to evapotranspiration, which becomes active after sunrise.

At 1400, the LH value for NOURBAN is higher than other scenarios (NOURBAN~400 Wm^{-2}, CONTROL~241 Wm^{-2}, GREEN~229 Wm^{-2}, and ALBEDO+GREEN~205 Wm^{-2}). ALBEDO had the same value as CONTROL. NOURBAN is the scenario that encompasses the

most natural vegetation state. Over the span of the daytime hours, it is evident that LH in GREEN is greater than CONTROL, which is expected. These results reflect the important role that vegetation surfaces play on the latent heat fluxes and by default, the surface energy equation latent heat fluxes and by default, the surface energy equation.

Figure 31 shows the time series for HFX. Similar to LH, all of the upward heat fluxes are closed to, or even below zero at night and begin an evolution similar to LH. At 1400, the HFX value for NOURBAN is the smallest, 175 Wm^{-2}. GREEN has the largest HFX value, 463 Wm^{-2}, followed by CONTROL, 396 Wm^{-2}, ALBEDO+GREEN, 293 Wm^{-2}. ALBEDO shows no difference from CONTROL. This result is quite confusing since HFX is considered as the index of sensible heat in this research and is expected to be more in line with the NOURBAN result. This result should be explored in more detail as non-linear responses, parameterization errors, or experiment set-up could be causing this unexpected result.

Figure 32 shows the time series for SWDOWN. It peaks at 1400 EDT. The values for five scenarios are very similar to each other. CONTROL shows a weak downward short wave flux (because of cloud forcing) at 1500 EDT, which can explain the low T2 at the same time for PDK.

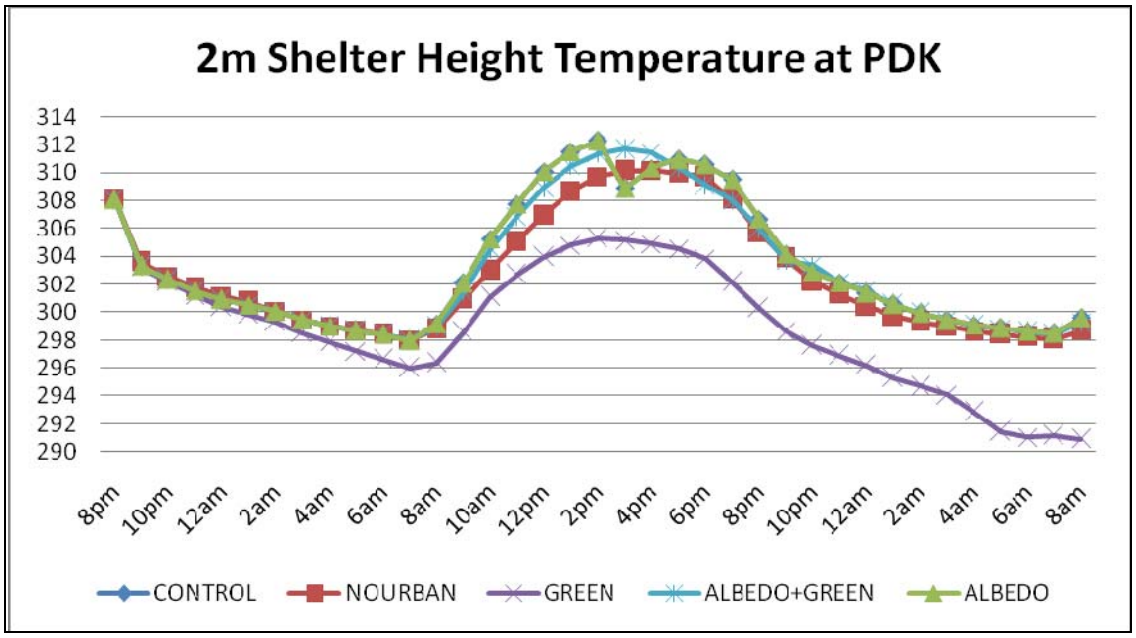

Figure 26 Time series of 2m shelter height temperature for five the five model scenarios

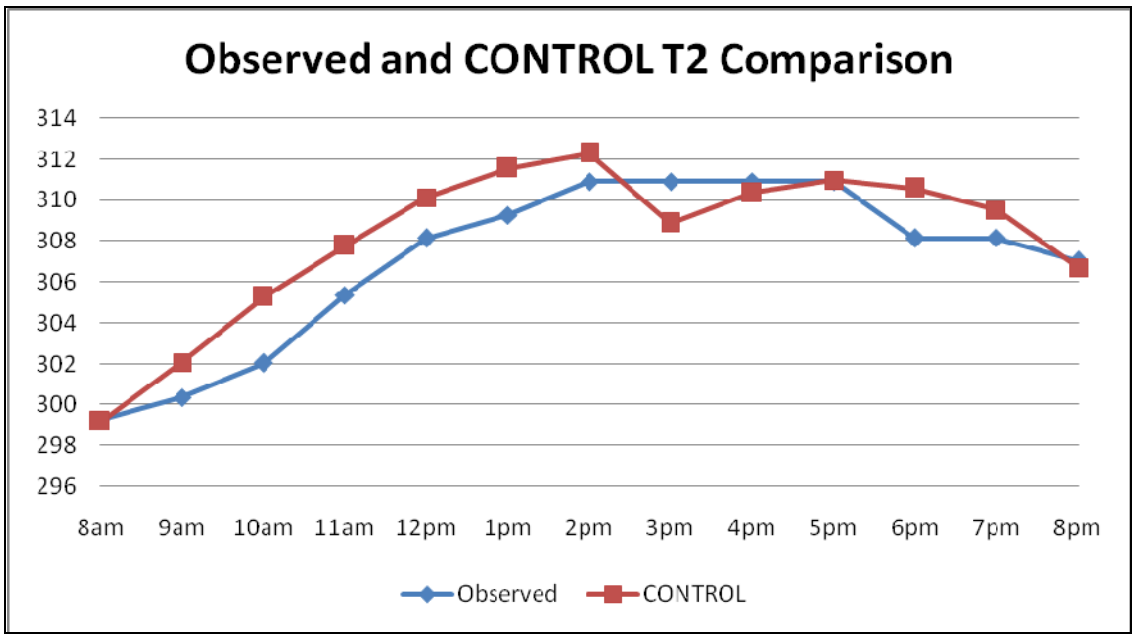

Figure 27 Observed and CONTROL 2m shelter height temperature comparison. 0800 to 2000 EDT 16 August 2007

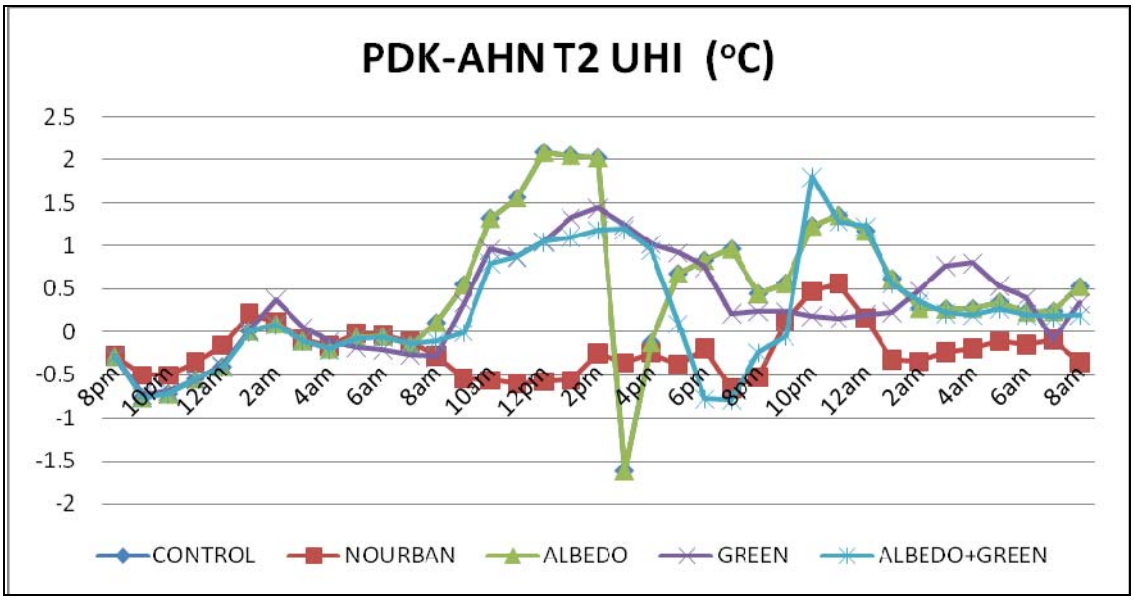

Figure 28 Time series of T2 PDK-AHN UHI for five model scenarios

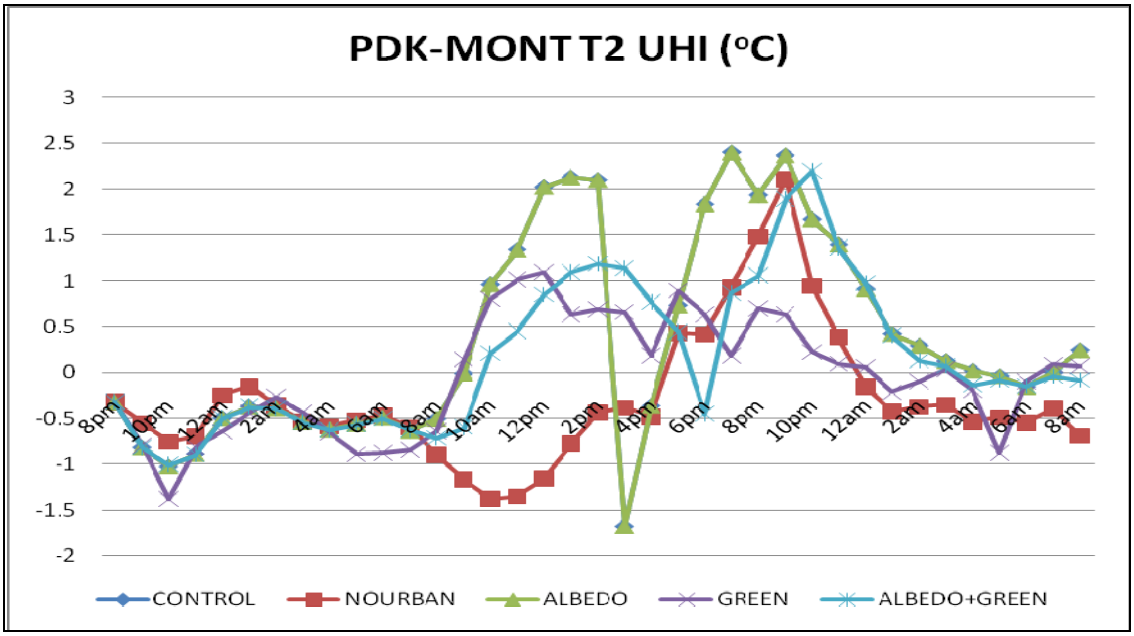

Figure 29 Time series of T2 PDK-MONT UHI for five model scenarios

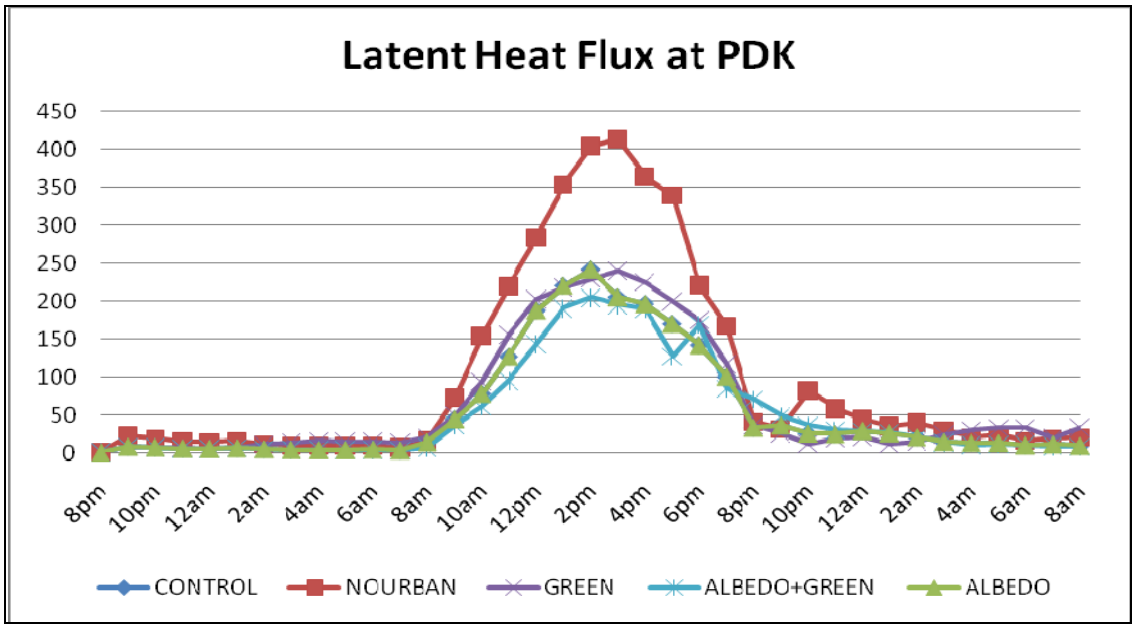

Figure 30 Time series of latent heat flux for five model scenarios

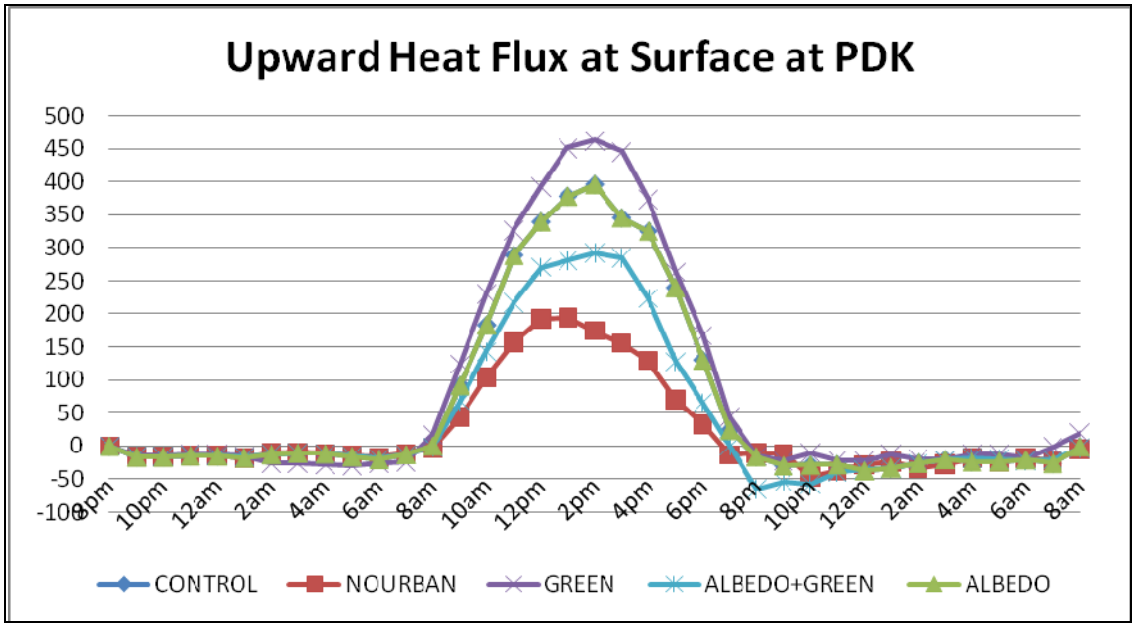

Figure 31 Time series of surface upward heat flux for five model scenarios

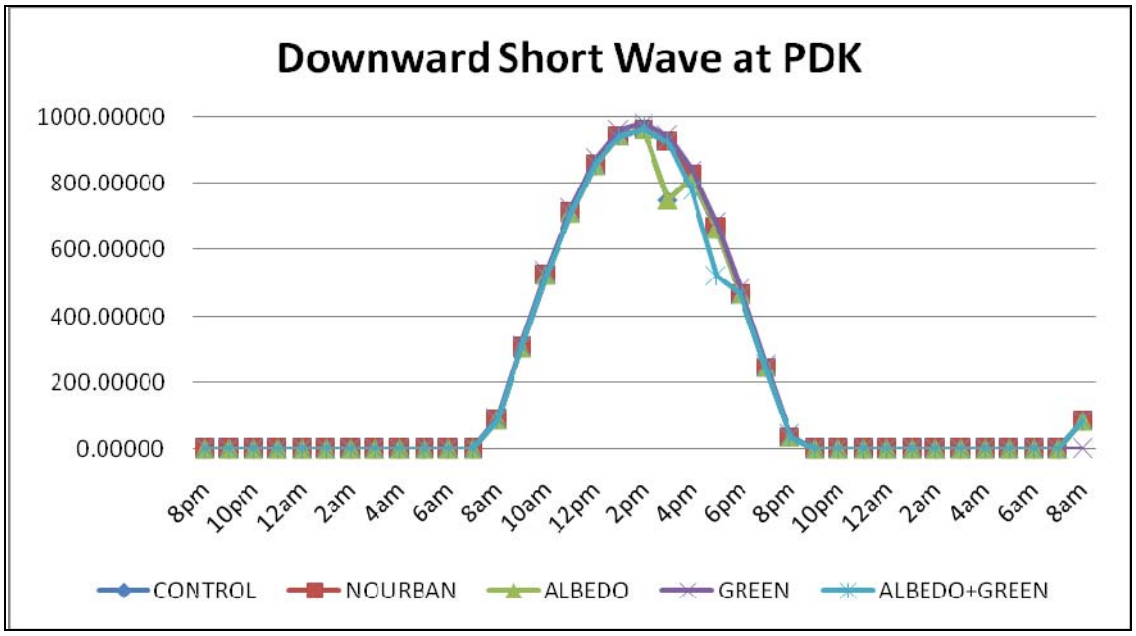

Figure 32 Time series of downward short wave flux for five model scenarios

CHAPTER 5

Conclusions

The annual minimum temperature trends for PDK, AHN, and MONT were calculated from *in situ* data. For PDK, no significant change was observed. For AHN, the minimum temperature trend was 0.70^{o}C per decade. And at MONT, there existed a significant negative trend of -1.79^{o}C per decade. This result can possibly be explained because Atlanta remained urban area during the study period, while Athens became more urban and Monticello stayed rural. MONT's decreased elevation may have contributed to its negative minimum temperature trend. However, the MONT trend initiation is not coincident with the elevation change years and there is no step-wise change.

A key finding of this study is that the mean UHI magnitide for PDK-AHN and PDK-MONT was 1.31^{o}C and 1.71^{o}C, respectively and these values are consistent with more limited model findings. This result provides a much needed climatological assessent of the Atlanta UHI. The annual UHI trends were tested before and after 1996, respectively. No significant change was observed in the pre- and post-1996 periods although the trends were significant for the entire period of the study record. As for the seasonal UHI, both PDK-AHN and PDK-MONT showed the largest UHI magnitudes in spring, and the smallest in summer. Cloud fraction data from MODIS provide compelling evidence that this could be a function of daytime cloud cover and radiative effects. Although, it should be emphasized that an exhaustive study was not intended. Other factors such as vegetation could certainly play a role in this seasonal UHI pattern.

In the heat wave climatology analysis, it was revealed that a heat wave in Atlanta occurred

during 50% of the years spanning 1984-2007. Atlanta heat waves occurred exclusively in the summer months and the mean number of heat waves events in Atlanta during a given heat wave year was 1.83. The results also revealed that, on average, Atlanta heat waves lasted 14.18 days although there was quite a bit of variability (standard deviation of 9.89). The mean maximum temperature during Atlanta's heat waves was 35.85° C. An important finding is that the PDK-MONT UHI intensity during heat wave days was much larger than that on non-heat wave summer days. The results suggested that the UHI in AHN and PDK are essentially the same regardless of whether a heat wave day is occurring or not.

From the five modeling ensembles - CONTROL, NOURBAN, ALBEDO, GREEN, and ALBEDO+GREEN, the following conclusions were drawn: (1) the modeling set-up accurately captured the evolution of the daytime and nocturnal heat island of Atlanta; (2) GREEN had the overall strongest effect on reducing two meter shelter height temperature. During the peak of the daytime UHI, a 100% in vegetation and evapotranspiration reduced temperature by as much as 7°; (3) a 100% increase in ALBEDO had essentially no effect on temperature and fluxes whereas a moderate (1 to 2 ° reduction at UHI peak) was found when ALBEDO was tripled; and (4) ALBEDO+GREEN had a cooling effect, but similar to previous studies, it was not as significant as individual changes.

Although GREEN was effective at decreasing surface temperature, we could not explain why its upward heat (sensible heat) would be larger than the CONTROL. This result merits further investigation. However, the latent heat flux and downward solar radiation values behaved as expected in the experiments.

From a mitigation and policy standpoint, our results suggests that tripling albedo can dramatically cool the city; however, unless there is a technological breakthrough in the future, it

is not easy to foresee how this could be achieved in Atlanta. Increased vegetation seems to be a feasible choice for mitigating surface temperature or some combination with high albedo surfaces. However, it is important for cities like Atlanta (or others) to consider whether surface or rooftop greening is more effective at reducing temperature. The results suggest that surface changes are important although we did not test elevated greening scenarios.

It is important to note that this model project did not consider urban roughness length, anthropogenic heating or aerosols. It also did not consider how density of the city could affect the proposed mitigation strategies. Detailed study, including the above conditions, may support (or refute) present findings. It is also worth noting that these experiments were intended to be theoretical. A future study should incorporate more "realistic" albedo and vegetation changes based on future urban planning projections in the Atlanta area. Additionally, more case studies with UHIs occurring at different times are also required. One limiting factor for Atlanta UHI studies that must be addressed in the future is the lack of detailed urban morphological parameters.

REFERENCES

Albany, N. Y., 2006: Mitigating New York City's Heat Island with Urban Forestry, Living Roofs, AND Light Surfaces New York City Regional Heat Island Initiative, 156 pp.

Beniston, M., 2004: The 2003 Heat Wave in Europe: A Shape of Things to Come? An Analysis Based on Swiss Climatological Data and Model Simulations. *Geophysical Research Letters*, **31,** 2022-2026.

Bornstein, R. D., and T. Oke, 1980: Influence of Pollution on Urban Climatology. *Advances in Environmental Sscience and Engineering.*, **3,** 171-202.

____, 1987: Mean Diurnal Circulation and Thermodynamic Evolution of Urban Boundary Layers. *Modeling the Urban Boundary Layer***,** 53–93.

____, and Q. Lin, 2000: Urban Heat Islands and Summertime Convective Thunderstorms in Atlanta: Three Case Studies. *Atmospheric Environment*, **34,** 507-516.

____, and Coauthors, 2006: Modeling the Effects of Land-use/Land-cover Modifications on the Urban Heat Island Phenomena in Houston, Texas. Final Report to David Hitchcock Houston Advanced Research Center, 100 pp.

Brazel, A., P. Gober, S. J. Lee, S. Grossman-Clarke, J. Zehnder, B. Hedquist, and E. Comparri, 2007: Determinants of Changes in the Regional Urban Heat Island in Metropolitan Phoenix (Arizona, USA) between 1990 and 2004. *Clim Res*, **33,** 171-182.

Changnon, S. A., K. E. Kunkel, and B. C. Reinke, 1996: Impacts and Responses to the 1995 Heat Wave: A Call to Action. *American Meteorological Society*, 1497-1506.

Dixon, P. G., and T. L. Mote, 2003: Patterns and Causes of Atlanta's Urban Heat Island–Initiated Precipitation. *Journal of Applied Meteorology*, **42,** 1273-1284.

EPA: What Can Be Done [Available online at http://www.epa.gov/hiri/strategies/index.html].

EPA: Trees and Vegetation [Available online athttp://www.epa.gov/hiri/strategies/vegetation.html]

Estes Jr, M., D. Quattrochi, and E. Stasiak, 2003: The Urban Heat Island Phenomenon: How Its Effects Can Influence Environmental Decision Making in Your Community. *Public Management (00333611)*, **85,** 8.

Ezber, Y., O. Lutfi Sen, T. Kindap, and M. Karaca, 2007: Climatic Effects of Urbanization in Istanbul: A Statistical and Modeling Analysis. *International Journal of Climatology*, **27,** 667.

Grimmond, C. S. B., and T. R. Oke, 1999: Heat Storage in Urban Areas: Local-Scale Observations and Evaluation of a Simple Model. *Journal of Applied Meteorology*, **38,** 922-940

Haffner, J., and S.Q. Kidder, 1999: Urban Heat Island Modeling in Conjunction with Satellite-derived Surface/soil Parameters. *J. Appl. Meteor.*, **38**, 448–465.

Ignatov, A., P. Minnis, N. Loeb, B. Wielicki, W. Miller, S. Sun-Mack, D. Tanré, L. Remer, I. Laszlo, and E. Geier, 2005: Two MODIS Aerosol Products over Ocean on the *Terra* and *Aqua* CERES SSF datasets. *J. Atmos. Sci.*, **62**, 1008–1031.

Jin, M., R. E. Dickinson, and D. Zhang, 2005: The Footprint of Urban Areas on Global Climate as Characterized by MODIS. *Journal of Climate*, **18,** 1551-1565.

____, J. M. Shepherd, and C. Peters-Lidard, 2007: Development of a Parameterization for Simulating the Urban Temperature Hazard Using Satellite Observations in Climate Model. *Natural Hazards*, **43,** 257-271.

Kalkstein, L. S., 1993: Health and Climate Change. Direct Impacts in Cities. *Lancet*, **342**, 8884, 1397-1399

Kim, Y.H., and J.J. Baik, 2002: Maximum Urban Heat Island Intensity in Seoul. *J. Appl. Meteor.*, **41**, 651–659.

Kunkel, K. E., S. A. Changnon, B. C. Reinke, and R. W. Arritt, 1996: The July 1995 Heat Wave in the Midwest: A Climatic Perspective and Critical Weather Factors. *Bulletin of the American Meteorological Society*, **77,** 1507-1518.

Kusaka, H., 2004: Simulation of the Urban Heat Island Effects over the Greater Houston Area With the High Resolution WRF/LSM/Urban Coupled System. *Simulation*, **1,** 4.

____., F. Kimura, H. Hirakuchi, and M. Mizutori, 2000: The Effects of Land-use Alteration on the Sea Breeze and Daytime Heat Island in the Tokyo Metropolitan Area. *J. Meteor. Soc. Japan,* **78,** 405–420.

Liptan, T., T. Miller, and A. Roy, 2004: Portland Ecoroof Vision: Quantitative Study to Support Policy Decisions. *Greening Rooftops for Sustainable Communities, Portland*.

Liu, Y., F. Chen, T. Warner, S. Swerdlin, J. Bowers, and S. Halvorson, 2004: Improvements to Surface Flux Computations in a Non-local-mixing PBL Scheme, and Refinements on Urban Processes in the Noah Land-surface Model with the NCAR/ATEC Real-time FDDA and Forecast System. *20th Conference on Weather Analysis and Forecasting/16th Conference on Numerical Weather Prediction.* 11-15 January, 2004, Seattle, Washington.

Manley, G., 1958: On the Frequency of Snowfall in Metropolitan England. *QJR Meteorol. Soc*, **84,** 70–72.

McKee, T. B., N. J. Doesken, C. A. Davey, and R. A. Pielke, Sr., 2000: Climate Data Continuity with ASOS, Report for Period April 1996 through June 2000. *Climatology Report 00-3, Dept. of Atmos. Sci., CSU, Fort Collins, CO, November*, 82 pp.

McPherson, E. G., 1994: Energy-saving Potential of Trees in Chicago. *Chicago's Urban Forest Ecosystem: Results of the Chicago Urban Forest Climate Project,* 95–114.

Meehl, G. A., and C. Tebaldi, 2004: More Intense, More Frequent, and Longer Lasting Heat Waves in the 21st Century. *Science*, **305,** 994-997.

Menne, B., 2003: The Health Impacts of 2003 Summer Heat-waves. *Briefing Note for the Delegations of the Fifty-third Session of the WHO Regional Committee for Europe. WHO Europe,* 12pp.

Mote, T.L., M.C. Lacke, J.M. Shepherd, 2007: Radar Signatures of the Urban Effect on Precipitation Distribution: A Case Study for Atlanta, Georgia. *Geophysical Res. Letters,* Vol. **34**, L20710,doi:10.1029/2007GL031903

United Nations., 2004: *World Urbanization Prospects: The 2003 Revision.* United Nations Publications, 335 pp.

NWS, 1995: Natural Disaster Survey Report: July 1995 Heat Wave. *Washington, DC: National Oceanic and Atmospheric Administration, National Weather Service, .*

Ohashi, Y., and H. Kida, 2002: Local Circulations Developed in the Vicinity of Both Coastal and Inland Urban Areas: A Numerical Study with a Mesoscale Atmospheric Model. *Journal of Applied Meteorology*, **41,** 30-45.

Oke, T. R., 1981: Canyon Geometry and the Nocturnal Urban Heat Island: Comparison of Scale Model and Field Observations. *J. Climatol*, **1,** 237–254.

——, 1982: The Energetic Basis of the Urban Heat Island. *Quarterly Journal of the Royal Meteorology Society*, **108,** 1-24.

Palecki, M. A, S. A. Changnon, K. E. Kunkel, 2001: The Nature and Impacts of the July 1999 Heat Wave in the Midwestern United States: Learning from the Lessons of 1995. *Bulletin of the American Meteorological Society*, **82**, 1353-1368.

Pfister, C., and Coauthors, 1999: Documentary Evidence on Climate in Sixteenth-Century Europe. Springer Science+ Business Media BV, Formerly Kluwer Academic Publishers BV, 55-110.

Quattrochi, D. A., J. C. Luvall, and M. G. Estes Jr, 1999: Project ATLANTA (Atlanta Land use Analysis: Temperature and Air Quality): Use of Remote Sensing and Modeling to Analyze How Urban Land Use Change Affects Meteorology and Air Quality Through Time. *NASA technical report*, **2147483647**.

____, and Coauthors, 1998: Project ATLANTA (ATlanta Land-use ANalysis: Temperature and Air quality): A Study of How the Urban Landscape Affects Meteorology and Air Quality through Time. *Preprints, Second Urban Environment Symposium*, **November** 2-6.

Rosenzweig, C., W. D. Solecki, L. Parshall, M. Chopping, G. Pope, and R. Goldberg, 2005: Characterizing the Urban Heat Island in Current and Future Climates in New Jersey. *Global Environmental Change B: Environmental Hazards*, **6,** 51-62.

Sailor, D.J., 1995: Simulated Urban Climate Response to Modifications in Surface Albedo and Vegetative Cover. *Journal of Applied Meteorology*, 34, 1694–1704.

____, Kalkstein, L. S, Wong, E, 2002: The Potential of Urban Heat Island Mitigation to Alleviate Heat-Related Mortality: Methodological Overview and Preliminary Modeling Results for Philadelphia. In *Proceedings of the 4th Symposium on the Urban Environment.* May 2002, Norfolk, Va., **4**:68-69.

____, 2003: Streamlined Mesoscale Modeling of Air Temperature Impacts of Heat Island Mitigation Strategies. Final report. Portland State University, 31pp

Schrumpf, A. D, 1996: Temperature Data Continuity with the Automatic Surface Observing System. *Thesis for the Degree of Master of Science, Department of Atmospheric Science, Colorado State University*. 256pp

Shepherd, J. M., H. Pierce, and A. J. Negri, 2002: Rainfall Modification by Major Urban Areas: Observations from Spaceborne Rain Radar on the TRMM Satellite. *Journal of Applied Meteorology*, **41,** 689-701.

____, O. O. Taylor, and C. Garza, 2004: A Dynamic GIS–Multicriteria Technique for Siting the NASA–Clark Atlanta Urban Rain Gauge Network. *Journal of Atmospheric and Oceanic Technology*, **21,** 1346-1363.

Skamarock, W. C., J. B. Klemp, and J. Dudhia, 2001: Prototypes for the WRF (Weather Research and Forecasting) model. Preprints. *Ninth Conf. on Mesoscale Processes*, 5pp.

Solecki, W. D., C. Rosenzweig, L. Parshall, G. Pope, M. Clark, J. Cox, and M. Wiencke, 2005: Mitigation of the heat island effect in urban New Jersey. *Global Environmental Change B: Environmental Hazards*, **6,** 39-49.

Souch, C., and S. Grimmond, 2006: Applied Climatology: Urban Climate. *Progress in Physical Geography*, **30,** 270-279.

Sterl, A., C. Severijns,H. Dijkstra,W. Hazeleger,G. Oldenborgh, M. Broeke, G. Burgers, B. Hurk, P. Leeuwen, and P. Velthoven, 2008: When Can We Expect Extremely High Surface Temperatures?, Geo. Res. Ltrs. (in press)

Taha, H., 1996: Modeling Impacts of Increased Urban Vegetation on Ozone Air Quality in the South Coast Air Basin. *Atmos. Environ.,* **30,** 3423–3430.

____, 1997: Modeling the Impacts of Large-scale Albedo Changes on Ozone Air Quality in the South Coast Air Basin. *Atmos. Environ.,* **31,** 1667–1676.

____, S. Douglas, and J. Haney, 1997: Mesoscale Meteorological and Air Quality Impacts of Increased Urban Albedo and Vegetation. *Energy and buildings*, **25,** 169-177.

____, 1999: Modifying a Mesoscale Meteorological Model to Better Incorporate Urban Heat Storage: A Bulk-parameterization Approach. *J. Appl. Meteor.*, **38**, 466–473.

Tewari, M., F. Chen, and W. Wang, 2004: Implementation and Verification of the Unified NOAH Land Surface Model in the WRF Model. *20thConference on Weather Analysis and Forecasting/16th Conference on Numerical Weather Prediction***,** 11-15.

Yang, X., and C. P. Lo, 2003: Modeling Urban Growth and Landscape Change for Atlanta Metropolitan Region. *International Journal of Geographical Information Science*, **17,** 463-488

Yoshino, M., 1975: Climate in a Small Area. University of Tokyo Press, Tokyo, Japan, 549 pp.